

## Chapter 4

### **Litho- and chemostratigraphy of the Johnnie Formation and Stirling Quartzite, Panamint Range and Funeral Mountains, eastern California: implications for the Death Valley record of Ediacaran ocean chemistry**

#### **ABSTRACT**

New carbon isotope data from thick exposures of the upper Johnnie Fm. in the Panamint Range of eastern California, combined with data from carbonate-rich facies of the Stirling Quartzite in the Funeral Mountains, provide a more complete record of  $\delta^{13}\text{C}$  fluctuations during the middle to late Ediacaran than previously determined from the Death Valley region. These data, coupled with field observations, provide evidence for at least three unconformities in the upper Johnnie Fm.: one at the base of the Johnnie oolite, a second, younger unconformity that is marked by a laterally extensive submarine debris flow in the central and northern Panamint Range, and a third unconformity at the Johnnie-Stirling contact. In the Funeral Mtns., carbonates in the uppermost Johnnie Fm. and in the lower part of the Stirling Quartzite have  $\delta^{13}\text{C}_{\text{PDB}}$  values near 0‰, suggesting that the Shuram anomaly is recorded entirely within the upper Johnnie Fm. and that previously recognized negative  $\delta^{13}\text{C}$  values from the middle to upper part of the Stirling Quartzite postdate the Shuram anomaly and predate the Precambrian-Cambrian boundary. Similarities in C isotope compositions suggest that incision of km-deep canyons in the Wonoka Fm. of South Australia could have been time equivalent with the submarine debris flow exposed in the Panamint Range.

## INTRODUCTION

The Johnnie Formation and Stirling Quartzite were deposited along the Cordilleran continental margin after the Marinoan cap carbonates of the underlying Noonday Dolomite (Prave, 1999, Petterson et al., 2007) and prior to the Precambrian-Cambrian boundary in the overlying Wood Canyon Fm. (Corsetti and Hagadorn, 2000). This time interval corresponds with the breakup of Rodinia and the development of the western Laurentian passive margin (e.g., Hoffman, 1991, Prave, 1999) and to some of the most significant geobiological events in earth history, including the radiation of multicellular organisms and the final stage in the oxygenation of the oceans (e.g., Fike et al., 2006, Kaufman et al., 2007, McFadden et al., 2008). Extremely light  $\delta^{13}\text{C}$  values from the upper part of the Johnnie Fm. (Corsetti and Kaufman, 2003) may record this final oxidation stage, and have been used to correlate the upper Johnnie Fm. with strata in Australia, Oman, and China (Halverson et al., 2005, Fike et al., 2006). Although it seems clear that previous geochemical studies in the Death Valley region have accurately located the stratigraphic position corresponding with the onset of this isotope excursion (e.g., Corsetti and Kaufman, 2003), a complete Death Valley C isotope record of the recovery from this event, which would include data from the upper Johnnie Fm. and possibly the overlying Stirling Quartzite, has not been assembled. Furthermore, the best Death Valley isotope data that do exist for this period come from one of the thinnest, most platformal settings in the region, raising the possibility that existing data do not fully capture  $\delta^{13}\text{C}$  fluctuations that may be recorded in thicker, more basinal settings. The association of older Neoproterozoic negative carbon isotope excursions with glaciations (e.g., Hoffman et al., 1998) coupled with geochronological evidence from

Newfoundland of a post-Marinoan glacial event (Bowring et al., 2003) has led to speculation of glacially-influenced sedimentation within the Johnnie Fm. (e.g., Abolins et al., 2000) which further motivates this study.

This paper reports the results of field and analytical work on the Johnnie Fm. and Stirling Quartzite conducted in the Panamint Range and Funeral Mountains of eastern California (Fig. 1). In the Panamint Range, the Johnnie Fm. is exposed continuously along strike for ~100 km, in contrast to more isolated exposures east of Death Valley where most studies of the Johnnie Fm. have been conducted. Field mapping and measured sections, as well as carbon isotope chemostratigraphy, from a ~30 km long transect in the Panamint Range (Fig. 2) were used to investigate along-strike facies changes within the upper Johnnie Fm. We also present new  $\delta^{13}\text{C}$  data from the uppermost Johnnie Fm. and lower Stirling Quartzite from carbonate-rich facies in the Funeral Mtns.

## **STRATIGRAPHIC AND TECTONIC SETTING**

The oldest Proterozoic stratigraphy in the southern Great Basin is the 3-4 km thick Pahrump Group, consisting of the Crystal Spring, Beck Spring, and Kingston Peak Formations (Fig. 3). U-Pb dates of 1.08 Ga from diabase sills that intrude the Crystal Spring Fm. (Heaman and Grotzinger, 1992) are the only reliable radiometric ages that have been determined from the Death Valley Proterozoic section, but correlations with other radiometrically dated sections worldwide have been facilitated by C isotope stratigraphy. Overlying the Kingston Peak Formation is the Noonday Dolomite, which was correlated by Prave (1999) to Marinoan cap carbonates (e.g., Kennedy, 1998) that

have subsequently been radiometrically dated at ~635 Ma in Namibia (Hoffmann et al., 2004) and China (Condon et al., 2005). Above the Noonday Dolomite are the Johnnie Formation, Stirling Quartzite, and Wood Canyon Formation. The trace fossil *Treptichnus pedum*, which first occurs in the lower Wood Canyon Fm., establishes the Precambrian-Cambrian boundary at this interval (Corsetti and Hagadorn, 2000). Deposition of the Noonday Dolomite to Lower Wood Canyon succession therefore may have occurred over as much as 90 to 100 My.

These sediments record the rifting history of southwest Laurentia and the subsequent development of a passive margin sequence. Structural and stratigraphic evidence of tectonism within the Kingston Peak Fm. (e.g., Walker et al., 1986) is generally considered to mark a period of rifting that was preceded by stable cratonic conditions and followed by development of the Cordilleran miogeocline (e.g., Stewart, 1972, Heaman and Grotzinger, 1986). Prave (1999) argued that Sturtian and Marinoan glacial deposits within the Kingston Peak Fm. correspond with two distinct periods of rifting. These field-based studies, which indicate that the “rift to drift” transition took place at approximately the Kingston Peak-Noonday contact, contrast with tectonic subsidence models which suggest that post-rift cooling began near 560 Ma (e.g., Bond et al., 1985), approximately 75 My after the Marinoan glaciation. Based on stratigraphic evidence from the Johnnie Fm., Summa (1993) concluded that it was deposited in subsiding basins related to extensional deformation, suggesting significantly younger rifting than previously thought and potentially reconciling the discrepancy between previous field

observations and subsidence models. Similarly, Clapham and Corsetti (2005) argued that there is evidence for tectonic activity at the Johnnie-Stirling contact.

The Panamint Range is an east-tilted fault block along the western margin of Death Valley that contains extensive exposures of all of the Proterozoic formations described above (e.g., Hunt and Mabey, 1966). The northern part of the range consists of a central area of greenschist to lower-amphibolite facies metamorphic rocks that is flanked on the east and west by normal faults carrying unmetamorphosed to greenschist-facies Proterozoic to Tertiary strata in their hanging walls (e.g., Hodges et al., 1990). The structurally lowest and regionally most persistent fault on the east side of the range where our work is concentrated is the middle Miocene Harrisburg Fault (Fig. 2), which typically places unmetamorphosed to weakly metamorphosed upper Johnnie Fm. onto higher-grade and stratigraphically lower units including the Kingston Peak Fm., Noonday Dolomite, and lower Johnnie Fm. (Wernicke et al., 1988, Hodges et al., 1990).

## **STRATIGRAPHY OF THE JOHNNIE FORMATION AND STIRLING QUARTZITE**

### **Background**

The Johnnie Fm., originally named by Nolan (1929) for exposures near Johnnie Wash in the Spring Mtns. (Fig. 1), lies disconformably on the underlying Noonday Dolomite (Summa, 1993). It varies in thickness from about 30 to 1600 m within the southern Great Basin (Stewart, 1970) and is comprised of siltstone, sandstone, dolostone, limestone and conglomerate. Stewart (1970) divided the Johnnie Fm. into the following six members,

listed in ascending order: transitional, quartzite, lower carbonate-bearing, siltstone, upper carbonate-bearing, and Rainstorm (Fig. 3). The uppermost of these, the Rainstorm Member (originally named by Barnes et al., 1965, for outcrops near the Rainstorm Mine in southern Nevada), is the most widespread across the southern Great Basin (Stewart, 1970) and is the primary focus of this study. As defined by Stewart (1970), the Rainstorm Member consists of basal siltstone overlain by a 1 to 2 m-thick oolite bed of regional extent (the so-called "Johnnie oolite") which is the most distinctive lithological feature within the Johnnie Fm. Overlying the Johnnie oolite is a thin siltstone interval that is typically followed by several meters of conspicuous pale red limestones and 50 to 80m of limey siltstones. Above this, the upper part of the Rainstorm Member varies widely in thickness from 15 to 200 m in previously described sections and is composed of siltstone, fine-grained sandstone, and occasional carbonates (Stewart, 1970). Summa (1993) conducted a detailed sequence stratigraphic study of the Johnnie Fm. which supplements the lithostratigraphic observations of Stewart (1970). She places a sequence boundary at the base of the Johnnie oolite, a flooding surface within the siltstones above the oolite, and another sequence boundary at the Johnnie-Stirling contact, as discussed below. She concluded from her work in the southern Nopah Range (Fig. 1) that the Johnnie Fm. there is comprised of a combination of shallow-marine and fluvial sediments and was deposited in an inner shelf basin. Rainstorm Member isopachs (Fig. 1, Stewart, 1970) illustrate NW or WNW thickening in three regions: 1) within the area immediately north of Las Vegas, 2) in an area that stretches along the Nevada-California border from approximately Clark Mtn. in the SE to the northern part of the Resting Spring Range in the NW, and 3) within the Panamint Range.

The contact relationship between the Johnnie Fm. and the overlying Stirling Quartzite has been the subject of some disagreement. Most early studies concluded that the contact is conformable (e.g., Stewart, 1970, Benmore, 1978), but in more recent investigations, Christie-Blick and Levy (1989) and Summa (1993) interpreted it as a sequence boundary and described incised valleys which locally removed as much as 150 m of the underlying Rainstorm Member before being filled with breccia and siltstone prior to deposition of the overlying Stirling Quartzite. Abolins et al. (2000) suggested that this canyon incision was related to glacioeustatic sea-level fall and that some of the clasts within the valley fill were derived from cap carbonates deposited subsequent to glaciation. Clapham and Corsetti (2005) argued against a glacial origin for the incised valleys and suggested that their locations were controlled by syndimentary normal faults.

Corsetti and Kaufman (2003) measured C isotopes in the Johnnie Fm. from sections in the southern Nopah Range, Alexander Hills, and Winters Pass Hills (Fig. 1). Their results revealed extremely light  $\delta^{13}\text{C}_{\text{PDB}}$  within Rainstorm Member carbonates (as negative as  $-11.5\text{‰}$ ), values which have subsequently been correlated with the early part of the so-called “Shuram anomaly” C isotope excursion in Oman, which is also known from several other sections worldwide (e.g., Halverson et al., 2005, Le Guerroué et al., 2006, Fike et al., 2006). The anomaly is manifest in most sections by an apparent rapid decline (relative to deposition rate) from positive values of  $\delta^{13}\text{C}$  to some of the lowest values ever recorded in the marine record, significantly below the mantle value of approximately  $-6\text{‰}$ . The values then gradually and monotonically recover to positive

values. The Shuram anomaly has been interpreted as the result of oxidation of large volumes of organic carbon in the deep ocean (Rothman et al., 2003, Fike et al., 2006, McFadden et al., 2008). In sections in Oman, South Australia, and China,  $\delta^{13}\text{C}_{\text{PDB}}$  of carbonates steadily increases from a nadir of about -12‰ up to 0‰ (Calver, 2000, Condon et al., 2005, Fike et al., 2006, McFadden et al., 2008). In contrast,  $\delta^{13}\text{C}_{\text{PDB}}$  from Rainstorm Member carbonates in the Winters Pass Hills (Corsetti and Kaufman, 2003; the most detailed data previously published from the Rainstorm Member) recover to only -9.2‰ below the contact with the Stirling Quartzite, suggesting that a significant part of the Shuram anomaly may be missing along the disconformity at the Johnnie-Stirling contact. The coincidence of the Johnnie oolite, which was probably deposited as a transgressive sheet following a period of erosion or non-deposition (Benmore, 1978, Summa, 1993, Kaufman et al., 2007), with the onset of the Shuram anomaly suggests that the events responsible for significantly altering the C isotope chemistry of the oceans at this time were associated with a rise in sea-level (Kaufman et al., 2007), not a fall as would be predicted from a glacial origin of the anomaly.

Global correlations of the Shuram anomaly, coupled with geochronological data from the Doushantuo Fm. in China and the Nafun Group in Oman, place some constraints on the age of the upper Johnnie Fm. and, in particular, the Johnnie oolite. Detrital zircons as young as 600 Ma from the Khufai Fm. in Oman (Le Guerroué et al., 2006) place a maximum age constraint on the onset of the Shuram anomaly and, by extension, deposition of the Johnnie oolite. A U-Pb date of  $551.1 \pm 0.7$  Ma from an ash bed in the upper part of the anomaly in the Doushantuo Fm. (Condon et al., 2005) provides a

minimum age constraint. Therefore, if correlations between these regions are valid, the implication is that the Johnnie oolite is between 551 and 600 My old. However, the most limiting U-Pb geochronological data from a single region are those of Condon et al. (2005) from China, which only bracket the age of the Shuram anomaly, and therefore the lower Rainstorm Member, between 551 and 633 Ma.

Much like the underlying Rainstorm Member, the Stirling Quartzite thickens to the NW or WNW and reaches a maximum thickness of >1600 m in southern Nevada (Fig. 9 of Stewart, 1970). It has been divided into five members, named, in ascending order, the A Member through E Member (Stewart, 1966, Stewart, 1970). Because carbonate beds are relatively rare in the Stirling Quartzite, C isotope data are sparse compared with other Neoproterozoic/Cambrian units in the region.  $\delta^{13}\text{C}$  data have previously been collected from the D Member in the Grapevine Mtns. and Bare Mtn. (Fig. 1, Corsetti and Hagadorn, 2000, Corsetti and Kaufman, 2003) and from the “middle member” in the southern Nopah Range and Salt Spring Hills (Fig. 1, Corsetti and Kaufman, 2003). Taken together, these data seem to suggest moderately negative values in the middle part of the formation which cross into positive values within the D Member (Corsetti and Hagadorn, 2000 and Corsetti and Kaufman, 2003).

### **Lithostratigraphy and C isotope data from the Panamint Range**

In the central and northern Panamint Range, the upper part of the Johnnie Fm. is lithostratigraphically distinct from the Rainstorm Member in the eastern Death Valley region. Although it contains siltstone and carbonate, it lacks the Johnnie oolite, pale red

limestones and abundant ripple marks and flute casts in fine-grained sandstones that distinguish the Rainstorm Member in the eastern Death Valley region and the southern Panamint Range. These dissimilarities have led to variable lithostratigraphic correlations and interpretations for these strata amongst previous workers (Hunt and Mabey, 1966, McDowell, 1967, Stewart, 1970, Benmore, 1978, Abolins et al., 2000).  $\delta^{13}\text{C}$  data from the Rainstorm Member, which reach primary values significantly lighter than at any other time in earth history, are particularly useful in this case for correlating various sections that have eluded definitive lithostratigraphic correlation. Here we describe 10 measured stratigraphic sections and accompanying C isotope data from the Panamint Range that span a total along-strike distance of 30 km. These data are presented in order from south to north, which also corresponds with lithofacies that are progressively unlike more thoroughly described sections of the Rainstorm Member to the east of Death Valley. C and O isotopic measurements were conducted in the stable isotope laboratories at Stanford University and the University of Michigan.

### ***Johnson Canyon***

In Johnson Canyon (Fig. 2), the upper Johnnie Formation is lithologically quite similar to exposures in the southern Nopah Range and many other locations east of Death Valley. Stewart (1970) recognized all six members of the Johnnie Fm in this area. The top and bottom of the Johnnie oolite contain rip-up clasts in outcrops examined in Johnson Canyon (Figs. 4 A and B), consistent with previous interpretations that the base of the oolite disconformably overlies the lower Rainstorm Member siltstones and marks the onset of a marine transgression (Summa, 1993, Kaufman et al., 2007), and possibly

suggesting another disconformity at the top of oolite. Scanning-electron microscope analysis of the oolite revealed numerous small ( $<100\ \mu\text{m}$ ) apatite crystals within both the ooids and micrite matrix. Attempts to measure U-Pb ages of these grains using isotope dilution-thermal ionization mass spectrometry were unsuccessful, however, because of insufficient radiogenic Pb. Immediately above the oolite are 5 m of siltstones overlain by 6.5 m of distinctive pale red limestones (Fig. 4C) similar in appearance to those described from the southern Nopah Range (e.g., Stewart, 1970, Summa, 1993, Corsetti et al., 2004). Above these are  $\sim 150\text{m}$  of siltstone and sandstone with rare, thin carbonate beds.

The total thickness of the Rainstorm Member in Johnson Canyon is  $\sim 160\ \text{m}$  (Fig. 5), approximately 2-3 times greater than in sections from the southern Nopah Range and Winters Pass Hills where previous C isotope studies have been conducted (Corsetti and Kaufman, 2003).  $\delta^{13}\text{C}_{\text{PDB}}$  within the upper carbonate bearing member vary somewhat but are generally 1 to 3‰ in the stratigraphically lowest samples (Fig. 5, Table 1). Values decrease up section and reach a value of -3.7‰ at the base of the Johnnie oolite. Within slightly over a meter, values decrease to -5.3‰ at the top of the Johnnie oolite (Fig. 5). In the overlying pale red limestones  $\delta^{13}\text{C}_{\text{PDB}}$  becomes even lighter, reaching a nadir of -11.6‰ near the top of these beds, nearly identical to the lightest values from dolostones above the Johnnie oolite in the Winters Pass Hills (Corsetti and Kaufman, 2003).  $\delta^{13}\text{C}_{\text{PDB}}$  values from Johnson Canyon show a slight overall increase in the overlying  $\sim 45\ \text{m}$  of section, reaching a value of -9.4‰. Siltstone and sandstone predominate in the upper  $\sim 100\text{m}$  of section, but thin dolostone beds record values no heavier than -7.3‰ beneath the contact with the Stirling Quartzite.

### ***South Fork of Hanaupah Canyon***

Along the South Fork of Hanaupah Canyon (Fig. 2), ~500m of limestone, dolostone, and siltstone underlie the Stirling Quartzite and overlie siltstones of the middle Johnnie Fm. (Fig. 6). McDowell (1967) was the first to describe the geology of this area in detail and defined this part of the section as the “limey argillite” member of the Johnnie Fm.

Within this interval and 180 m below the contact with the Stirling Quartzite are ~7 m of edgewise conglomerate (Fig. 4D), previously noted by McDowell (1967) and Stewart (1970). Three lithostratigraphic correlations have been proposed for this section of the upper Johnnie Fm. Stewart (1970) and Benmore (1978) interpreted it as the Rainstorm Member, a suggestion which is supported by previous descriptions of a 1.4 m-thick oolite bed at the base of the section (Benmore, 1978). Although we did not find oolite in the section we measured, we have observed isolated exposures of probable Johnnie oolite as far north as Trail Canyon (described below) and suspect the oolite could have easily been omitted by erosion or non-deposition over much of the central and northern Panamints.. McDowell (1967) made the same correlation but suggested that the edgewise conglomerate, located in the upper half of the limey argillite member, was equivalent to the Johnnie oolite, which normally occurs near the base of the Rainstorm Member (e.g., Stewart, 1970). Abolins et al. (2000) suggested that the edgewise conglomerate was deposited within a canyon that was incised into the top of the Rainstorm member.

$\delta^{13}\text{C}_{\text{PDB}}$  values from carbonates within this section are approximately -10‰ at the bottom and decrease fairly regularly up section to about -5‰ near the top (Fig. 5). Three

samples from the matrix of the edgewise conglomerate have  $\delta^{13}\text{C}_{\text{PDB}}$  ranging from -7.6 to -8.5‰. The similarity of these limey argillite member values with data from the Rainstorm Member in Johnson Canyon support the interpretation of Stewart (1970) and Benmore (1978) that the entire ~500 m of section is equivalent to the Rainstorm Member. These data also suggest that deposition of the edgewise conglomerate postdates the Johnnie oolite, which has  $\delta^{13}\text{C}_{\text{PDB}}$  of -3.7 to -5.3‰ in Johnson Canyon and corresponds with the rapidly decreasing part of the Shuram anomaly, not the gradually increasing part. The absence of a discernable change in  $\delta^{13}\text{C}$  within the matrix of the edgewise conglomerate or within overlying sediments argues against the interpretation of Abolins et al. (2000) that the conglomerate was deposited above a major unconformity. It is also noteworthy that  $\delta^{13}\text{C}_{\text{PDB}}$  of carbonates reach values as heavy as -5.2‰ at the top of this section, compared with the heaviest value of -7.3 ‰ from Johnson Canyon.

#### ***North Fork of Hanaupah Canyon***

From Hanaupah Canyon to the Wildrose Peak area (Fig. 2), unusual occurrences of carbonates at the Johnnie-Stirling contact were noted by Hunt and Mabey (1966) and mapped by Albee et al. (1981) but have not previously been investigated in detail. The largest and best exposed outcrop of these is found in the north fork of Hanaupah Canyon, where ~100 m of dolostone is situated between fine-grained sandstones and siltstones of the Johnnie Fm. below and sandstones of the Stirling Quartzite above (Fig. 7A). In detail, this outcrop consists of cross-bedded dolostone and carbonate breccia in the lower 2.5 m (Fig. 8A), overlain by 0.5 m of stromatolitic fine-grained dolostones (Fig. 8B) which, in some ways, resemble the tubestones of the underlying Noonday Dolomite (e.g.,

Cloud et al., 1974). Lying above the stromatolitic dolostone are 11 m of carbonate breccia, sandstone, and conglomerate and an additional 11 m of laminated dolostone and siltstone. The remainder of the section is comprised of 75 m of sandy dolostone containing stromatolites with up to 0.5m of synoptic relief (Fig. 8C). The top of the carbonate section is brecciated, and the contact with the overlying Stirling Quartzite is sharp.

The contact of this carbonate unit with underlying sandstones and siltstones is well exposed in the north fork of Hanaupah Canyon. A thin, white sandstone in the area is a useful marker bed for illustrating the stratigraphic relationship between the carbonate unit and underlying and overlying strata. Along the south wall of the canyon (Figs. 7B and C) this marker bed is separated from the overlying Stirling Quartzite by 2 m of sandy, cross-bedded dolostone. Tracing the marker bed to the east, it is down-dropped by a steeply east-dipping normal fault which also offsets beds in the overlying Stirling Quartzite. Just to the east of this fault, the carbonate unit is significantly thicker than in the footwall and reaches its full thickness of 100 m within a couple of hundred meters to the north where the white quartzite bed is still present at the base (Fig. 7A). The carbonate unit appears to thin to almost zero thickness farther to the north before intersecting another fault (Fig. 7A). The overall picture is therefore of a lens-shaped carbonate unit, 2.5 km in length, thickest in the middle and tapering to zero thickness to the north and south.

$\delta^{13}\text{C}$  values are significantly different in this 100 m-thick section than in sections of upper Rainstorm Member described previously (Fig. 5). The stratigraphically lowest

sample has carbonate  $\delta^{13}\text{C}_{\text{PDB}}$  of -4.5‰, and values increase in the overlying 20 m of section to -3.3‰ before increasing suddenly to ~0‰. In the uppermost 80 m of section they increase slightly to as much as 1.2‰. These values thus contrast with  $\delta^{13}\text{C}$  from the upper Johnnie Fm. in the south fork of Hanaupah Canyon and in Johnson Canyon, being wholly greater than even the heaviest isotopes in the uppermost Johnnie Fm in the other sections.

### ***Wildrose Peak area***

Albee et al. (1981) mapped a thin dolostone unit at the top of the Johnnie Fm. from the north fork of Hanaupah Canyon to the vicinity of Wildrose Peak (Fig. 2). This unit, “jud: Johnnie upper dolostone” on the map of Albee et al. (1981), includes the thick carbonate unit in the north fork of Hanaupah Canyon described above as well as thinner dolostones to the north that are at a similar stratigraphic position. We mapped the northern reaches of the dolostone along strike for about 4 km, starting 0.5 km east of the Thorndike campground and proceeding north (Figs. 2 and 9). In the southern part of this transect, the dolostone is overlain by sandstones of the Stirling Quartzite, and to the north siltstones pinch in between it and the Stirling Quartzite. The dolostone becomes discontinuous in the northernmost km of the transect, either from faulting, overall poor exposure, or stratigraphic pinch out.

This unit generally consists of light grey to white, laminated dolostone and lesser limestone, and becomes sandier up section. Where we measured it, the unit is 40m thick, although this seems to vary somewhat along-strike. Where exposed, the base is

frequently brecciated, and breccias occur throughout the section. In one particularly good exposure of the upper 4 m of the unit, the lower 2m consists of brecciated sandy dolostone overlain by laminated dolostone and siltstone. Above this is 1 m of dolostone with domal stromatolites, followed by 50 cm of planar laminated dolostone. Overlying the dolostone are several tens of meters of dark grey siltstone followed by sandstone of the Stirling Quartzite. In another good exposure of the top of the carbonate unit 1 km to the north, the overall stratigraphy is similar, consisting of a laminated uppermost part underlain by carbonate intraformational breccia. In this area, giant ooids (Sumner and Grotzinger, 1993), ~1 cm in diameter (Fig. 8D), occur in a thin interval between the breccia and overlying laminated dolostone.

Carbon isotope samples were collected from several locations within this unit, and we have combined the results to create a composite chemostratigraphy (Fig. 5).  $\delta^{13}\text{C}_{\text{PDB}}$  of carbonate at the base of the unit is -3.5‰, increases sharply to near 0‰ within the middle, and then increases more gradually to values as great as 1.8‰ in the upper portion. The two exposures of the top of the unit described above yield similar results:  $\delta^{13}\text{C}_{\text{PDB}}$  of carbonate from the brecciated portion are between 1.2 and 1.7‰, and values are -0.1 to 1.5‰ in the overlying laminated and oolitic dolostones. The giant ooids have a  $\delta^{13}\text{C}_{\text{PDB}}$  value of 0.2‰. Although thinner than the carbonate unit described from the north fork of Hanaupah Canyon,  $\delta^{13}\text{C}$  values of these dolostones are generally similar.

### *Trail Canyon*

The majority of our work was conducted in Trail Canyon (Figs. 2 and 10), where the Johnnie Fm. is well exposed along strike for 8 km in an area of high relief. For the purpose of mapping, the Johnnie Fm. in this area is best divided into three members. The lower member (Zjl) consists predominantly of dark-grey siltstone with lesser carbonate and is separated from the underlying Noonday Dolomite by a fault in most of Trail Canyon. Based on our mapping (Fig. 11), we estimate a thickness of 330 m for this member. Above Zjl are some 200m of light-green siltstones and orange- to brown-weathering, laminated, silty dolostones comprising the middle member (Zjm).

The contact between Zjm and the overlying upper member (Zju) is defined by a carbonate breccia horizon that can be followed nearly continuously from the road leading to Aguerberry Point in the north to the southern end of the south fork of Trail Canyon, a distance of at least 8 km (Fig. 11). The most common clast type within the breccia is a distinctive bluish grey limestone. During reconnaissance in Blackwater Wash (Fig. 2), located an additional 5 km to the north, the breccia bed was found at the same stratigraphic position and with similar clast composition (Figs. 12A and B). Blocks within the breccia that have discernable edges at outcrop scale can reach up to 10m in diameter (Fig. 13), and the largest blocks are at least 10s of meters in length. In many places, 3 m of laminated, sandy dolostone occurs within the breccia (Fig. 14A). The presence of limestone clasts both above and below this laminated dolostone make it difficult to determine whether the laminated dolostone beds are themselves large clasts. Bedding in the laminated dolostone is always parallel to bedding above and below the

breccia, however, providing some indication that it may be autochthonous and was deposited synchronously with the allochthonous blocks in the breccia bed. To the south the breccia bed becomes thicker and very sandy, reaching a thickness of 85 m in the south fork of Trail Canyon.

Above the breccia bed, Zju is composed almost entirely of dark-grey siltstone with occasional thin dolomitic beds. In places we have observed thin-bedded alternations of siltstone and fine-grained sandstone within Zju, which we interpret as turbidites (Fig. 14B). Two thin conglomerate beds occur in the uppermost part of Zju (Stewart, 1970, Abolins et al., 2000) and are usually composed of quartz granules and pebbles (Fig. 14C), although they may also contain siltstone clasts. We measured a thickness of 281 m for Zju, and our estimate for the combined thickness of Zjm, the breccia bed, and Zju within the northern part of Trail Canyon is 490 m. The abrupt change in lithology across the breccia bed, from siltstones and thin-bedded carbonates in Zjm to almost entirely siltstones in Zju, suggests an unconformity between these units at the level of the breccia bed. As described below, all previously published C isotope data from the Johnnie Fm. come from stratigraphic positions significantly below this intra-Rainstorm unconformity.

The central and eastern portions of Trail Canyon comprise an east-dipping homocline of the units described above and the overlying Stirling Quartzite, Wood Canyon Formation, Zabriskie Quartzite, and Carrera Fm. (Fig. 11). It is cut by numerous, relatively small, generally south-dipping normal faults that cut at high angles across bedding, as well as shallowly north-dipping normal faults with greater offset. The western part of the area is

made up of highly deformed Noonday Dolomite and, in places, overlying Zjl siltstone. In the western area the Noonday-Johnnie contact is offset by a series of east-dipping, high-angle normal faults (Figs. 10 and 11). Separating the western area from the central and eastern areas is an east-dipping normal fault of considerable offset which, according to the generalized geologic maps of Hodges et al. (1987) and Hodges et al. (1990), is the southern continuation of the Harrisburg Fault. In the northern part of the Trail Canyon area this fault juxtaposes Zjl and the Noonday Dolomite; in the middle part it drops Zjm onto the Noonday, and in the southern part it separates Zjm in the hanging wall from Zjl in the footwall (Fig. 11). To the south of the mapped area, vegetation and extremely rugged topography obscure the transition to the upper Johnnie section near Wildrose Peak described in the previous section.

C isotope data were obtained from six measured sections within Trail Canyon. The southernmost section is in the south fork of Trail Canyon (location TC1, Fig. 11), where the lower 39 m are in siltstones and laminated and cross-bedded dolostones of Zjm, and stratigraphically higher samples are from 85 m of carbonate breccia and coarse-grained dolomitic sandstone which underlie siltstones of Zju. Dolostones in the upper part of Zjm have  $\delta^{13}\text{C}_{\text{PDB}}$  values ranging from -10.6 to -11.0‰ (Fig. 15), which are typical for carbonates in the lower part of the Rainstorm Member, above the oolite. Above Zjm,  $\delta^{13}\text{C}_{\text{PDB}}$  in the carbonate breccia/dolomitic sandstone interval are strikingly different, falling between -0.7 and 1.1‰.

The next section to the north begins in Zjm and includes two large limestone blocks from the breccia bed separating Zjm and Zju (location TC2, Figs. 11 and 13). About 25 m below the breccia bed, a dolostone bed records  $\delta^{13}\text{C}_{\text{PDB}}$  of -4.6‰, and ~3m below the breccia bed values reach as heavy as about -2.1‰ (Fig. 15). Above these, one sample was collected from a relatively small breccia block which has a  $\delta^{13}\text{C}_{\text{PDB}}$  value of 1.2‰ (Fig. 15). In the overlying, larger block, seven samples were collected which range from -3.6‰ at the “base” to 1.0‰ at the “top,” although the facing direction within the block could not be determined.

To the north, samples were collected from carbonates overlying the diamictite locality described by Abolins (1999) in the central portion of Trail Canyon (location TC3, Fig. 11). Our mapping indicates that the diamictite, overlying limestones and carbonate breccias in this area are all part of the breccia bed separating Zjm and Zju. The diamictite (Fig. 14D) is underlain by Zjm siltstones and consists of pebble- to boulder-size limestone clasts supported by a silty matrix. It is overlain by 7 m of massive sandy limestone which is brecciated at its base, and which we interpret as an allochthonous block. Above this are 14 m of matrix- and clast- supported carbonate breccia followed by another block of black, sandy limestone that is overlain by Zju siltstones.  $\delta^{13}\text{C}_{\text{PDB}}$  in the lower limestone block is -1.8‰ at the base and increase to -0.4‰ near the middle before decreasing again to -1.9‰ at the top (Fig. 15). The upper limestone has  $\delta^{13}\text{C}_{\text{PDB}}$  of 1.5‰ at the base, decreasing to -2.7‰ at the top. The pattern in this block is similar to that in the block at TC1, except inverted.

An intact section of lower Johnnie Fm. and possibly uppermost Noonday Dolomite is exposed near the detachment fault in the northern part of this area (location TC4, Fig. 11). The basal 12 m of this section is primarily grey, laminated to massive dolostone overlain by dolostone containing thin siltstone beds. It is unclear if these beds are lower Johnnie Fm. or upper Noonday Dolomite. Above these carbonates are 11 m of siltstones followed by a 9 m-thick breccia bed containing carbonate clasts supported in a silty matrix (Fig 16 A and B). Overlying the breccia are 29 m of siltstones with an increasing number of thin dolostone beds up-section. In the 30 m of section above these siltstones, at least 4 rhythmic cycles are developed which each consist of a basal bed of silty, laminated dolostone, an intermediate bed of pure, thin-bedded dolostone, and upper siltstone beds (Fig. 16C), which we interpret as deepening-upward. Overlying the siltstones of the last cycle there is a very distinctive, 6 m-thick horizon of siltstone supporting dispersed rounded carbonate boulders up to 1.5 m in diameter (Fig. 16D). Lying above the “boulder horizon” are ~250 m of siltstone and rare carbonates which make up the majority of Zjl, and these are followed concordantly by Zjm.  $\delta^{13}\text{C}_{\text{PDB}}$  from the basal carbonate part of section TC4 vary from about -2 to -4‰ (Fig. 15), comparable to values from the lower Johnnie Fm. in the southern Nopah Range (Corsetti and Kaufman, 2003) and from the upper Noonday Dolomite (Prave, 1999, Corsetti and Kaufman, 2003).  $\delta^{13}\text{C}_{\text{PDB}}$  of carbonate from the dolostone-siltstone cycles is broadly similar, varying from about -2.5 to -3.7‰.

The northernmost section is just south of the road leading to Aguerberry Point (location TC5, Fig. 11) and includes samples collected from the base of Zjm through the upper part

of Zju (Fig. 15). The two stratigraphically lowest carbonate samples from Zjm have  $\delta^{13}\text{C}_{\text{PDB}}$  of -6 to -9‰, and slightly above these, a thin oolite bed records values of about -10 to -11‰. In the upper part of Zjm,  $\delta^{13}\text{C}_{\text{PDB}}$  of carbonate is as heavy as -4‰, and  $\delta^{13}\text{C}_{\text{PDB}}$  of carbonate in the matrix of the overlying breccia bed is also about -4‰. Carbonate beds are rare within the Zju siltstones, but those that are present indicate that  $\delta^{13}\text{C}_{\text{PDB}}$  values return to more negative values, approximately -6 to -7‰, in the lower part of Zju.

Finally, we collected samples from the lower part of the D member of the Stirling Quartzite near Trail Canyon (location TC6, Fig. 5).  $\delta^{13}\text{C}_{\text{PDB}}$  is -5.2‰ at the base of the D Member (Fig. 15), increases slightly to about -4.2‰, and then decreases to about -6.4‰ in the highest carbonate bed we sampled 30 m above the base of the D member. The total thickness of the D member in this area is approximately 125m (Stewart, 1970).

### **Lithostratigraphy and C isotope data from the Funeral Mountains**

With the exception of the upper dolostone unit in Hanaupah Canyon, the uppermost Johnnie Fm. and most of the Stirling Quartzite are siliciclastic in the Panamint Range, in the Funeral Mtns. (Fig. 1) more abundant carbonate beds in this interval provide an opportunity to measure  $\delta^{13}\text{C}_{\text{carb}}$  above and below the Johnnie-Stirling contact. We collected samples from two locations: near Indian Pass in the northern part of the Funeral Mtns. and near Lees Camp in the central part (Fig. 1). In the Indian Pass area, a 2 m-thick bed of sandy dolostone is situated in the uppermost part of the Johnnie Fm. (Wright and Troxel, 1993). Unlike the dolostone at the Johnnie-Stirling contact in the central

Panamint Range described above, the dolostone bed near Indian Pass is not brecciated and has gradational upper and lower contacts. We have seen no evidence that it is allochthonous. Near Indian Pass another dolostone interval, approximately 13 m thick, is used as a marker horizon within the A Member of the Stirling Quartzite (Wright and Troxel, 1993). In the Lees Camp area, a sandy dolostone bed of comparable thickness is found in the A Member (Stewart, 1970, Wright and Troxel, 1993), and is presumed to be equivalent to the bed near Indian Pass. Near Lees Camp, the middle and upper parts of the Stirling Quartzite contain much more carbonate than in most other locations. Both Stewart (1970) and Wright and Troxel (1993) mapped at least portions of the Lees Camp area, and they differ somewhat in their conventions for identifying various members of the Stirling Quartzite. Below, we follow the descriptions and mapping of Stewart (1970) when referring to the C and D Members.

$\delta^{13}\text{C}_{\text{PDB}}$  from the upper Johnnie Fm. dolostone near Indian Pass ranges from -0.7 to 1.6‰, and the Stirling A marker horizon in this area records broadly similar values of -1.7 to 0.2‰ (Fig. 17A). In the Lees Camp area, the Stirling A carbonate marker bed has  $\delta^{13}\text{C}_{\text{PDB}}$  values of -2 to 0.3‰, essentially indistinguishable from values to the north.  $\delta^{13}\text{C}_{\text{PDB}}$  of carbonate from the overlying C and D members of the Stirling Quartzite are significantly different from these values, however. Values in the lower part of the C member are -3.6 to -4.3‰ and become heavier upsection, crossing 0‰ in the D member (Fig. 17B), consistent with previous data from the Grapevine Mtns. (Corsetti and Hagadorn, 2000).

## **DISCUSSION AND CONCLUSIONS**

### **Correlations within the Panamint Range**

Sections of the upper Johnnie Fm. in Johnson Canyon (the “conventional” Rainstorm Member lithologically similar to the type section in Nevada and sections in the eastern Death Valley region), the south fork of Hanaupah Canyon (the limey argillite member), and the northernmost part of Trail Canyon (Zjm and Zju) are lithologically quite dissimilar and therefore difficult to correlate based strictly on lithostratigraphy.

However, distinctive C isotope data from these areas may be used to establish correlation between various sections.

Based on our C isotope data, we correlate the 160 m of typical Rainstorm Member lithologies exposed in Johnson Canyon with the upper 500 m of the Johnnie Fm in the north fork of Hanaupah Canyon and with Zjm from section TC4 in Trail Canyon (Fig. 18). Because our data from Hanaupah Canyon do not definitively record the onset of the Shuram anomaly, we cannot confidently correlate the base of the Rainstorm Member to these areas. Furthermore, Stewart (1970) measured a thickness of only 280 m for the Rainstorm Member in the south fork of Hanaupah Canyon. He noted that because of numerous small faults, his estimate for the true thickness was uncertain, and it is unclear if he measured his section in the same location we did. Our measured thickness also suffers from uncertainty due to faulting and should be treated with some caution.

We interpret the breccia bed in Trail Canyon as a submarine gravity flow or “olistostrome” (e.g., Krause and Oldershaw, 1979). Relatively heavy  $\delta^{13}\text{C}$  values from within the breccia bed in the southern part of Trail Canyon (locations TC1-3, Figs. 5 and 11) contrast markedly with values measured in strata immediately below (locations TC1, 2 and 4) and above (location TC4) the breccia. The original stratigraphic positions of the large blocks are difficult to ascertain because their C isotope values, though rapidly changing through the two mlarger blocks, are non-unique. The prevalence of fine-grained siliclastics, turbidites, and debris flows within the Johnnie Fm. in Trail Canyon suggest deeper water deposition than at localities to the southeast such as the southern Nopah Range (Summa, 1993).

Our mapping near the Thorndike campground suggests that the dolostones and breccias found at the Johnnie-Stirling contact from the north fork of Hanaupah Canyon to near Wildrose Peak, i.e., the “Johnnie upper dolostone” unit of Albee et al. (1981), are equivalent to the breccia bed in Trail Canyon. In the area of our map transect near the campground, the dolostone unit is overlain by sandstone of the Stirling Quartzite to the south and progressively more siltstone (equivalent to Zju) to the north (Fig. 9). In Trail Canyon, the thickness of Zju siltstone overlying the breccia bed reaches 280 m and becomes even thicker in the northernmost Panamint Range. If these beds are, in fact, equivalent, one implication is that the limey argillite member in the south fork of Hanaupah Canyon correlates with Zjm in Trail Canyon. C isotope data from these locations (Figs. 5 and 15) are consistent with this interpretation:  $\delta^{13}\text{C}_{\text{PDB}}$  of carbonate from the limey argillite member range from -10.5‰ at the base to approximately -5‰ at

the top, while in the TC4 section,  $\delta^{13}\text{C}_{\text{PDB}}$  reaches a nadir of -10.9‰ near the base of Zjm and increases to -4‰ at the top, just below the breccia bed. The difference in thickness between these units can probably be attributed to accumulation rate, which seems to have been significantly greater near Hanaupah Canyon than at Trail Canyon.

Assuming that transport of the gravity flow was roughly north-south, a minimum run out distance of ~22 km is suggested by our field observations, spanning from the north fork of Hanaupah Canyon in the south to Blackwater Wash in the north (Fig. 2). The stratigraphic relationship between the breccia bed and the overlying Stirling Quartzite provides strong evidence that the Johnnie-Stirling contact is a sequence boundary. In the southern Panamint Range and to the southeast of Death Valley, this sequence boundary is a disconformity at the Johnnie-Stirling contact, while in more basinal locations such as Trail Canyon and the Funeral Mtns. it is either a slight disconformity or a correlative conformity. Assuming further that the base of the Stirling Quartzite is isochronous, we can estimate the slope on which the breccia bed was deposited from the along-strike distance between the south fork of Hanaupah Canyon, where the base-of-Stirling unconformity has just eroded through the breccia bed, to the north end of Trail Canyon (location TC4), where 280 m of Zju is present between the breccia bed and the overlying unconformity (Fig. 19). This distance is ~17 km, from which we estimate a northward-dipping slope of approximately 1 degree.

The significance of the 100 m-thick carbonate bed in the north fork of Hanaupah Canyon (Fig. 7) is still a matter of some uncertainty. As described above, this bed has a carbonate

breccia at its base (Fig. 8A), is also brecciated at the top, and forms a discontinuous outcrop that pinches out to the north and south. Based on these observations it is tempting to conclude that it is a giant olistolith, some 2.5 km in length, located in an up-dip position within the breccia bed. Geochemical data from the bed are inconclusive on this matter:  $\delta^{13}\text{C}$  values are entirely heavier than in the limey argillite member in the south fork of Hanaupah Canyon, located only a short distance to the south, and are actually somewhat similar to those from the middle part of the Noonday Dolomite (Pettersen et al., 2007). On the other hand, the slightly positive values from the upper part of the bed are similar to those found in the uppermost Johnnie Fm. near Indian Pass (Fig. 17A), suggesting that the bed could be autochthonous. Regardless, we consider the brecciated upper portion of this bed and the sharp contact with the overlying Stirling Quartzite to be convincing evidence for an unconformity at the top of the unit and note that its thickness may have originally been greater but was eroded prior to deposition of the Stirling Quartzite.

#### **Record of the Shuram anomaly in the Death Valley region**

C isotope data from the Winters Pass Hills (Corsetti and Kaufman, 2003), where the Rainstorm Member is 80 m thick (Stewart, 1970), have been used to correlate the upper Johnnie Fm. with strata in Oman, China, and Australia (Halverson et al., 2005, Fike et al., 2006). In light of the evidence for a sequence boundary at the Johnnie-Stirling contact, it is reasonably clear that only the earliest part of the Shuram anomaly is preserved in the Winters Pass Hills. As one progresses from southeast to northwest across the Death Valley region, a greater proportion of the Shuram anomaly is preserved beneath the

unconformity at the Johnnie-Stirling contact, as illustrated by increasingly heavy  $\delta^{13}\text{C}$  values from the uppermost Johnnie Fm. In the Winters Pass Hills, the Rainstorm Member reaches values no heavier than  $-9.2\text{‰}$  beneath the contact with the Stirling Quartzite (Corsetti and Kaufman, 2003). In Johnson Canyon, the heaviest values near the top of the Johnnie Fm. are  $-7.3\text{‰}$ . In the south fork of Hanaupah Canyon, they become as heavy as  $-5.2\text{‰}$ . In Trail Canyon, they are  $-2.3\text{‰}$ . Finally, near Indian Pass, the top of the Johnnie Fm. records  $\delta^{13}\text{C}_{\text{PDB}}$  values of 0 to  $1.5\text{‰}$  (Figs. 1 and 18). Data from the Johnnie Fm. in Trail Canyon and near Indian Pass thus suggest that  $\delta^{13}\text{C}_{\text{PDB}}$  of carbonate returned to values at or near  $0\text{‰}$  prior to deposition of the Stirling Quartzite, a conclusion which is supported by some slightly positive  $\delta^{13}\text{C}$  values from the Stirling A member in the Indian Pass and Lees Camp areas of the Funeral Mtns. If one assumes relatively isochronous deposition of individual members of the Stirling Quartzite across the Death Valley region, negative values from the Stirling C and D members documented in this paper and by Corsetti and Hagadorn (2000) and Corsetti and Kaufman (2003) suggest that an additional negative isotope excursion occurred during deposition of the lower part of the Stirling Quartzite.

Our data from Zju at location TC4 indicates that following the recovery of  $\delta^{13}\text{C}_{\text{PDB}}$  to about  $-4\text{‰}$  during deposition of Zjm, values decreased to about  $-6$  to  $-7\text{‰}$  at the base of Zju, just above the breccia bed, and recovered to at least  $-2.3\text{‰}$  in overlying Zju sediments. This spike does not seem to have been recognized in any other sections worldwide, and unfortunately the evidence for it in the Panamint Range is quite limited due to the lack of carbonate in Zju. At location TC2, two dolostone beds in the upper

part of Zjm have carbonate  $\delta^{13}\text{C}_{\text{PDB}}$  of -4.6 and -2.1‰, providing additional evidence of recovery to relatively heavy values prior to emplacement of the breccia bed. Some corroborating evidence for an additional recovery prior to deposition of the Stirling Quartzite is provided by  $\delta^{13}\text{C}_{\text{PDB}}$  values of 2.6 to 2.9‰ in samples of a thin limestone bed deposited within incised channels at the Johnnie-Stirling contact in the southern Nopah Range (Corsetti and Kaufman, 2003). These values, which postdate the Johnnie oolite and predate the Stirling Quartzite, suggest that the recovery of the Shuram anomaly to positive values ended before deposition of the Stirling Quartzite. In the following section we discuss the only other known section with clear evidence for an unconformity at a similar stratigraphic position.

### **Comparison with the Wonoka Formation, South Australia**

The Shuram anomaly has also been identified in the Wonoka Fm. in the Adelaide Geosyncline of South Australia (Calver, 2000). In this area, incised valleys, up to ~1 km deep, were eroded into the lower Wonoka Fm. and underlying strata and were subsequently filled prior to deposition of the overlying Bonney Sandstone (e.g., von der Borch, 1982). Whether the incision and filling of these canyons required subaerial exposure has been the matter of some debate (e.g., von der Borch et al., 1989), as have the origin of the canyons. Explanations for canyon incision include lowering of sea-level in a restricted basin due to evaporation (e.g., Christie-Blick et al., 1990) and uplift related to a mantle plume (Williams and Gostin, 2000).

C isotope data from Calver (2000) can be utilized to investigate the relative timing of incision and filling of the Wonoka canyons. In the central part of the Flinders Ranges in South Australia, where there is no evidence of canyon incision,  $\delta^{13}\text{C}_{\text{PDB}}$  of carbonate is slightly less than 0‰ at the base of the Wonoka Fm., decreases rapidly to a nadir of -11.2‰ 90 m up section, and then recovers back to 0‰ near the top of the formation (Fig. 20, Calver, 2000). This overall pattern is very similar to that recognized in the Shuram and Buah Fms. in Oman (Fike et al., 2006). The stratigraphic position of the unconformity that correlates with the base of the canyons has been estimated to be at one of two levels within this section (Fig. 20, Christie-Blick et al., 1990, Christie-Blick et al., 1995). Importantly, if either of these correlations is correct, it implies that the most negative values of the Shuram anomaly preceded the incision of the Wonoka Canyons and  $\delta^{13}\text{C}_{\text{PDB}}$  of carbonate subsequently recovered to at least -8‰ before incision of the canyons. In the northern part of the Flinders Ranges, where the Wonoka canyons are developed,  $\delta^{13}\text{C}_{\text{PDB}}$  of carbonate ranges from -6.7 to -8.2‰ in the lower ~1100 m of canyon fill (Fig. 20, Calver, 2000).

Comparison of C isotope data from the Wonoka Fm. with our new data from the Panamint Range illustrates an interesting possible correlation.  $\delta^{13}\text{C}_{\text{PDB}}$  of carbonate at the top of the limey argillite member in the south fork of Hanaupah Canyon reaches values as heavy as -5.2‰ beneath the contact with the Stirling Quartzite (Fig. 5). As outlined above, our mapping suggests that the top of this member is equivalent to the top of Zjm in Trail Canyon, which reaches values as heavy as about -4‰.  $\delta^{13}\text{C}_{\text{PDB}}$  values from the base of Zju are -6.5 to -7.2‰ (Fig. 15), comparable to values from the fill within

the Wonoka Canyons. We note that based on available data, it is possible that the unconformity and breccia bed within the Rainstorm Member identified during this study correlate with the unconformity marking the base of the Wonoka canyons. In this scenario, Zjm preserves a slightly later record of C isotope compositions than has been measured below the sub-canyon unconformity in the Wonoka Fm., while the bottom part of Zju and the base of the canyon fill are at least roughly isochronous.

## REFERENCES

- Abolins, M.J., 1999, I. Stratigraphic constraints on the number of discrete Neoproterozoic glaciations and the relationship between glaciation and Ediacaran evolution. II. The Kwichup Spring thrust in the northwestern Spring Mountains, Nevada: implications for large-magnitude extension and the structure of the Cordilleran thrust belt [Ph.D. thesis]: Pasadena, California Institute of Technology, 340 p.
- Abolins, M., Oskin, R., Prave, T., Summa, C., and Corsetti, F., 2000, Neoproterozoic glacial record in the Death Valley region, California and Nevada, *in* Lageson, D.R., Peters, S.G., and Lahren, M.M., eds., Great Basin and Sierra Nevada: Boulder, Geological Society of America Field Guide 2, p. 319-335.
- Albee, A.L., Labotka, T.C., Lanphere, M.A., and McDowell, S.D., 1981, Geologic map of the Telescope Peak quadrangle, California: U.S. Geological Survey Geologic Quadrangle Map GQ-1532, scale 1:62,500, 1 sheet.

Barnes, H., Christiansen, R.L., and Byers, F.M. Jr., 1965, Geologic map of the Jangle Ridge quadrangle, Nye and Lincoln Counties, Nevada: U.S. Geological Survey Geologic Quadrangle Map GQ-363, scale 1:24,000, 1 sheet.

Benmore, W.C., 1978, Stratigraphy, sedimentology, and paleoecology of the late Paleophytic or earliest Phanerozoic Johnnie Formation, eastern California and southwestern Nevada [Ph.D. thesis]: Santa Barbara, University of California, 243 p.

Bond, G.C., Christie-Blick, N., Kominz, M.A., and Devlin, W.J., 1985, An early Cambrian rift to post-rift transition in the Cordillera of western North America: *Nature*, v. 315, p. 742-746.

Bowring, S.A., Myrow, P.M., Landing, E., Ramezani, J., and Grotzinger, J.P., 2003, Geochronological constraints on terminal Neoproterozoic events and the and the rise of metazoans: *Geophysical Research Abstracts*, 5, 13219.

Calver, C.R., 2000, Isotope stratigraphy of the Ediacarian (Neoproterozoic III) of the Adelaide Rift Complex, Australia, and the overprint of water column stratification: *Precambrian Research*, v. 100, p. 121-150.

Calver, C.R., and Lindsay, J.F., 1998, Ediacarian sequence and isotope stratigraphy of the Officer Basin, South Australia, *Australian Journal of Earth Sciences*, v. 45, p. 513-532.

Christie-Blick, N., Dyson, I.A., and von der Borch, C.C., 1995, Sequence stratigraphy and the interpretation of Neoproterozoic earth history: *Precambrian Research*, v. 73, p. 3-26.

Christie-Blick, N., and Levy, M., 1989, Stratigraphic and tectonic framework of upper Proterozoic and Cambrian rocks in the western United States, *in* Christie-Blick, N., and Levy, M., eds., *Late Proterozoic and Cambrian tectonics, sedimentation, and record of Metazoan radiation in the western United States*: Washington, D.C., American Geophysical Union, Field Trip Guidebook T331, p. 7-21.

Christie-Blick, N., von der Borch, C.C., and DiBona, P.A., 1990, Working hypotheses for the origin of the Wonoka Canyons (Neoproterozoic), South Australia: *American Journal of Science*, v. 290A, p. 295-323.

Clapham, M.E., and Corsetti, F.A., 2005, Deep valley incision in the terminal Neoproterozoic (Ediacaran) Johnnie Formation, eastern California, USA: tectonically or glacially driven?: *Precambrian Research*, v. 141, p. 154-164.

Cloud, P., Wright, L.A., Williams, E.G., Diehl, P., and Walter, M.R., 1974, Giant stromatolites and associated vertical tubes from the upper Proterozoic Noonday Dolomite, Death Valley region, eastern California: *Geological Society of America Bulletin*, v. 85, p. 1869-1882.

Condon, D., Zhu, M., Bowring, S., Wang, W., Yang, A., and Jin, Y., 2005, U-Pb ages from the Neoproterozoic Doushantuo Formation, China: *Science*, v. 308, p. 95-98.

Corsetti, F.A., and Hagadorn, J.W., 2000, Precambrian-Cambrian transition: Death Valley, United States: *Geology*, v. 28, p. 299-302.

Corsetti, F.A., and Kaufman, A.J., 2003, Stratigraphic investigations of carbon isotope anomalies and Neoproterozoic ice ages in Death Valley, California: *Geological Society of America Bulletin*, v. 115, p. 916-932.

Corsetti, F.A., Lorentz, N.J., and Pruss, S.B., 2004, Formerly-aragonite seafloor fans from Neoproterozoic strata, Death Valley and southeastern Idaho, United States: implications for “cap carbonate” formation and snowball Earth, *in* Jenkins, G.S., et al., eds., *The Extreme Proterozoic: Geology, Geochemistry, and Climate*. American Geophysical Union Geophysical Monograph Series, v. 146, Washington, DC, p. 33–44.

Eickhoff, K.-H., von der Borch, C.C., and Grady, A.E., 1988, Proterozoic canyons of the Flinders Ranges (South Australia): submarine canyons or drowned river valleys?: *Sedimentary Geology*, v. 58, p. 217-235.

Fike, D.A., Grotzinger, J.P., Pratt, L.M., and Summons, R.E., 2006, Oxidation of the Ediacaran ocean: *Nature*, v. 444, p. 744-747.

Halverson, G.P., Hoffman, P.F., Schrag, D.P., Maloof, A.C., and Rice, A.H.N., 2005, Toward a Neoproterozoic composite carbon-isotope record: Geological Society of America Bulletin, v. 117, p. 1181-1207.

Harding, M.B., 1987, The geology of the Wildrose Peak area, Panamint Mountains, California [Ph.D. thesis]: Laramie, University of Wyoming, 207 p.

Heaman, L.M., and Grotzinger, J.P., 1992, 1.08 Ga diabase sills in the Pahrump Group, California: implications for development of the Cordilleran miogeocline: Geology, v. 20, p. 637-640.

Hodges, K.V., Walker, J.D., and Wernicke, B.P., 1987, Footwall structural evolution of the Tucki Mountain detachment system, Death Valley region, southeastern California, *in* Coward, M.P., et al., eds., Continental Extensional Tectonics: Oxford, Geological Society Special Publication No. 28, p. 393-408

Hodges, K.V., McKenna, L.W., and Harding, M.B., 1990, Structural unroofing of the central Panamint Mountains, Death Valley region, southeastern California, *in* Wernicke, B.P., ed., Basin and Range extensional tectonics near the latitude of Las Vegas, Nevada: Geological Society of America Memoir 176, Boulder, p. 377-390.

Hoffman, P.F., 1991, Did the breakout of Laurentia turn Gondwanaland inside-out?: Science, v. 252, p. 1409-1412.

Hoffman, P.F., Kaufman, A.J., Halverson, G.P., and Schrag, D.P., 1998, A Neoproterozoic snowball Earth: *Science*, v. 281, p. 1342-1346.

Hoffmann, K.-H., Condon, D.J., Bowring, S.A., and Crowley, J.L., 2004, U-Pb zircon date from the Neoproterozoic Ghaub Formation, Namibia: constraints on Marinoan glaciation: *Geology*, v. 32, p. 817-820.

Hunt, C.B., and Mabey, D.R., 1966, Stratigraphy and structure, Death Valley, California: U.S. Geological Survey Professional Paper 494-A, 162 p.

Kaufman, A.J., Corsetti, F.A., and Varni, M.A., 2007, The effect of rising atmospheric oxygen on carbon and sulfur isotope anomalies in the Neoproterozoic Johnnie Formation, Death Valley, USA: *Chemical Geology*, v. 237, p. 47-63.

Kennedy, M.J., Runnegar, B., Prave, A.R., Hoffmann, K.-H., and Arthur, M.A., 1998, Two or four Neoproterozoic glaciations?: *Geology*, v. 26, p. 1059-1063

Krause, F.F., and Oldershaw, A.E., 1979, Submarine carbonate breccia beds-a depositional model for two-layer sediment gravity flows from the Sekwi Formation (Lower Cambrian), Mackenzie Mountains, Northwest Territories, Canada: *Canadian Journal of Earth Sciences*, v. 16, p. 189-199.

Le Guerroué, E., Allen, P.A., Cozzi, A., Etienne, J.L., and Fanning, M., 2006, 50 Myr recovery from the largest negative  $\delta^{13}\text{C}$  excursion in the Ediacaran ocean: *Terra Nova*, v. 18, p. 147-153.

McDowell, S.D., 1967, The intrusive history of the Little Chief granite porphyry stock, central Panamint Range, California: I. Structural relationships. II. Petrogenesis, based on electron microprobe analyses of the feldspars [Ph.D. thesis]: Pasadena, California Institute of Technology, 282 p.

McFadden, K.A., Huang, J., Chu, X., Jiang, G., Kaufman, A.J., Zhou, C., Yuan, X., and Xiao, S., 2008, Pulsed oxidation and biological evolution in the Ediacaran Doushantuo Formation: *Proceedings of the National Academy of Sciences*, v. 105, p. 3197-3202.

Nolan, T.B., 1929, Notes on the stratigraphy and structure of the northwest portion of Spring Mountain, Nevada: *American Journal of Science*, v. 17, p. 461-472.

Petterson, R., Prave, A., Wernicke, B., and Fallick, A.E., 2007, New stratigraphic and isotopic constraints on the Cryogenian-Ediacaran strata of Death Valley region, *Geological Society of America Abstracts with Programs*, v. 39, no. 6, p. 222.

Prave, A.R., 1999, Two diamictites, two cap carbonates, two  $\delta^{13}\text{C}$  excursions, two rifts: the Neoproterozoic Kingston Peak Formation, Death Valley, California: *Geology*, v. 27, p. 339-342.

Rothman, D.H., Hayes, J.M., and Summons R.E., 2003, Dynamics of the Neoproterozoic carbon cycle: Proceedings of the National Academy of Sciences, v. 100, p. 8124-8129.

Stewart, J.H., 1966, Correlation of lower Cambrian and some Precambrian strata in the southern Great Basin, California and Nevada: U.S. Geological Survey Professional Paper 550C, p. C66-C72.

Stewart, J.H., 1970, Upper Precambrian and lower Cambrian strata in the southern Great Basin, California and Nevada: U.S. Geological Survey Professional Paper 620, 206 p.

Stewart, J.H., 1972, Initial deposits in the Cordilleran geosyncline: evidence of a late Precambrian (<850 m.y.) continental separation: Geological Society of America Bulletin, v. 83, p. 1345-1360.

Summa, C.L., 1993, Sedimentologic, stratigraphic, and tectonic controls of a mixed carbonate-siliciclastic succession: Neoproterozoic Johnnie Formation, southeast California [Ph.D. thesis]: Cambridge, Massachusetts Institute of Technology, 332 p.

Sumner, D.Y., and Grotzinger, J.P., 1993, Numerical modeling of ooid size and the problem of Neoproterozoic giant ooids: Journal of Sedimentary Petrology, v. 63, p. 974-982.

von der Borch, C.C., Grady, A.E., Eickhoff, K.H., Dibona, P., and Christie-Blick, N., 1989, Late Proterozoic Patsy Springs Canyon, Adelaide geosyncline: submarine or subaerial origin?: *Sedimentology*, v. 36, p. 777-792.

von der Borch, C.C., Smit, R., and Grady, A.E., 1982, Late Proterozoic submarine canyons of Adelaide geosyncline, South Australia: *American Association of Petroleum Geologists Bulletin*, v. 66, p. 332-347.

Walker, J.D., Klepacki, D.W., and Burchfiel, B.C., 1986, Late Precambrian tectonism in the Kingston Range, southern California: *Geology*, v. 14, p. 15-18.

Wernicke, B.P., Walker, J.D., and Hodges, K.V., 1988, Field guide to the northern part of the Tucki Mountain fault system, Death Valley region, California, *in* Weide, D.L., and Faber, M.L., eds., *This extended land, geological journeys in the southern Basin and Range*, Geological Society of America Cordilleran Section Field Trip Guidebook, p. 58-63.

Williams, G.E., and Gostin, V.A., 2000, Mantle plume uplift in the sedimentary record: origin of kilometre-deep canyons within late Neoproterozoic successions, South Australia: *Journal of the Geological Society, London*, v. 157, p. 759-768.

Wright, L.A., and Troxel, B.W., 1993, Geologic map of the central and northern Funeral Mountains and adjacent areas, Death Valley region, southern California: U.S. Geological Survey, Miscellaneous Investigations Series Map I-2305, scale 1:24,000, 1 sheet.

**FIGURE CAPTIONS**

**Figure 1.** Shaded relief map of part of the southern Great Basin showing locations mentioned in text and thickness (in feet) of the Rainstorm Member of the Johnnie Fm. Isopachs from Stewart (1970).

**Figure 2.** Shaded relief map of the Panamint Range showing study locations, Miocene detachment faults, and location of the Johnnie Fm. Sources of mapping: Hunt and Mabey (1966), McDowell (1967), Albee et al. (1981), Harding (1987), this study, and unpublished mapping from R. Petterson, C. Verdel, and B. Wernicke. Fault locations from Hodges et al. (1990). Abbreviations: EF-Emigrant Fault, HF-Harrisburg Fault.

**Figure 3.** Generalized Proterozoic to earliest Cambrian stratigraphy of the Death Valley region.

**Figure 4.** Photographs from Johnson Canyon and the south fork of Hanaupah Canyon. (A) Breccia at the base of the Johnnie oolite, Johnson Canyon. (B) Breccia at the top of the Johnnie oolite, Johnson Canyon. (C) Pink limestones above the Johnnie oolite, Johnson Canyon. (D) Edgewise conglomerate in upper Johnnie Fm., south fork of Hanaupah Canyon.

**Figure 5.** C isotope data for the upper Johnnie Fm. from sections measured in Johnson Canyon, Hanaupah Canyon, and near Wildrose Peak. Datum for Johnson Canyon section is within the upper carbonate-bearing member. N. fork Hanaupah Canyon and Wildrose

Peak data are from dolostones in the uppermost Johnnie Fm. Position of the Johnnie oolite in the N. fork of Hanaupah Canyon is approximated from the description of Benmore (1978). Note differences in vertical scales. Abbreviations: jud-Johnnie upper dolostone, Zj-undifferentiated Johnnie Fm., Zju-upper Johnnie Fm., Zsa-A member, Stirling Quartzite.

**Figure 6.** North-looking photograph of upper Johnnie Fm. and lower Stirling Quartzite along the south fork of Hanaupah Canyon. Width of view in the foreground is approximately 1.6 km.

**Figure 7.** Upper Johnnie Fm. dolostone in the N. fork of Hanaupah Canyon. (A) Photograph looking northeast into the N. fork. Dashed line marks the contact between the dolostone and the overlying Stirling Quartzite. Note white marker bed below the dolostone. (B) Photograph looking south at the south wall of the N. fork of Hanaupah Canyon showing the southern termination of the dolostone. Width of view in the middle ground is ~250 m. (C) Sketch illustrating stratigraphic relationships between the dolostone, underlying Johnnie Fm., and overlying Stirling Quartzite. Abbreviations: jud-Johnnie upper dolostone, Zs-Stirling Quartzite, Zj-Johnnie Fm.

**Figure 8.** Photographs of upper Johnnie Fm. carbonates, Hanaupah Canyon to Wildrose Peak. (A) Breccias at base of the dolostone in the N. fork of Hanaupah Canyon. (B) Stromatolites (tubes?) near base of dolostone unit, N. fork of Hanaupah Canyon. (C)

Stromatolites in the upper part of dolostone unit, N. fork Hanaupah Canyon. (D) Giant ooids in upper Johnnie Fm. carbonates, near Wildrose Peak.

**Figure 9.** Geologic map of the Johnnie-Stirling contact near Wildrose Peak.

**Figure 10.** Photograph looking north into Trail Canyon. Detachment fault is probably the continuation of the Harrisburg Fault. Fig. 11 is a geologic map of this area.

Abbreviations: Zn-Noonday Dolomite, Zjl-lower Johnnie Fm., Zjm-middle Johnnie Fm., Zju-upper Johnnie Fm., Zs-Stirling Quartzite, CZw-Wood Canyon Fm., Cz-Zabriskie Quartzite.

**Figure 11.** Geologic map of the Trail Canyon area showing locations of measured sections TC 1 through 6. Contour interval is 50 meters.

**Figure 12.** Johnnie Fm. breccia bed in Blackwater Wash. (A) Photograph looking north at section of Johnnie Fm. and lower Stirling Quartzite. Width of view in foreground is approximately 300 meters. (B) Breccia clast of blue-grey limestone.

**Figure 13.** Giant limestone breccia clasts in Trail Canyon at location TC2. Circle around ~1.8m-tall person for scale.

**Figure 14.** Photographs of the upper Johnnie Fm. in Trail Canyon. (A) Laminated dolostone within breccia bed, near location TC5. (B) Thin-bedded alternations of

siltstone and fine-grained sandstone, interpreted as turbidites, near location TC3. (C) Quartz granules and pebbles in upper Johnnie Fm. (D) Carbonate clasts in siltstone matrix, near base of section measured at location TC3.

**Figure 15.** Carbon isotope data from sections measured in the Trail Canyon area. We interpret carbonates in the TC3 section and upper parts of the TC1 and TC2 sections as allochthonous blocks. Note that vertical scale of TC4 and TC5 sections is different than other sections.

**Figure 16.** Photographs of the lower Johnnie Fm. in Trail Canyon. (A) Limestone clasts in breccia near base of Zjl. (B) Matrix-supported carbonate clasts, same breccia near base of Zjl. (C) Deepening-upward cycles, as indicated by arrows. Circle around rock hammer for scale. (D) Rounded carbonate boulders supported in a silty matrix.

**Figure 17.** Carbon isotope data from sections measured in the Funeral Mtns.

**Figure 18.** Johnnie Fm. carbon isotope data from the Winters Pass Hills, Johnson Canyon, the S. fork of Hanaupah Canyon, and the northern part of the Trail Canyon area. Datum for Winters Pass Hills section is the base of the Noonday Dolomite (Corsetti and Kaufman, 2003). Position of the Johnnie oolite in the N. fork of Hanaupah Canyon is approximated from the description of Benmore (1978). Position of the Johnnie oolite at location TC5 is taken as the oolite bed near the base of the section.

**Figure 19.** Scale drawing of Zjm/Zju/breccia illustrating possible correlation between middle and upper Johnnie Fm. sediments in Hanaupah Canyon and Trail Canyon.

**Figure 20.** Summary of carbon isotope data from the Wonoka Fm., south Australia.

Figure 1

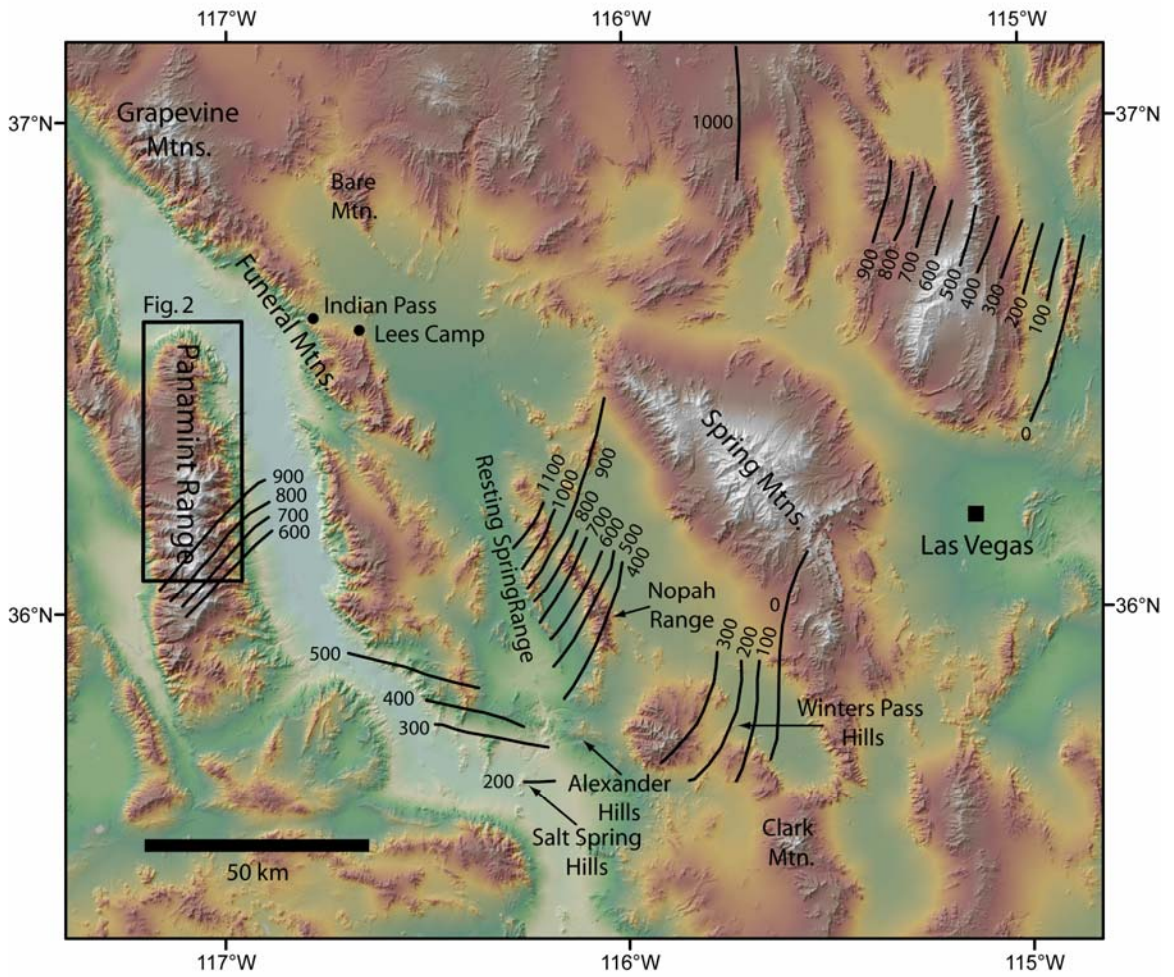


Figure 2

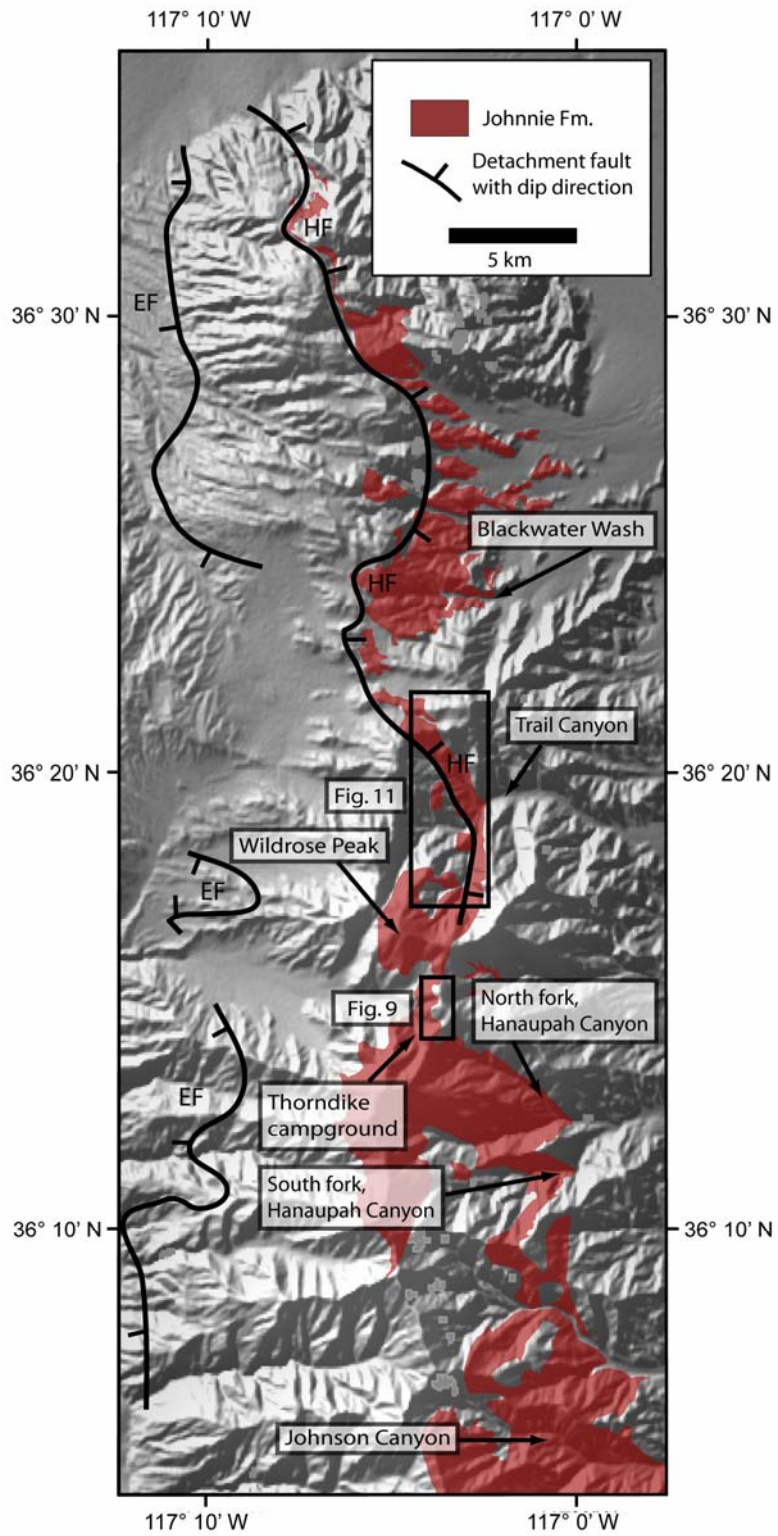


Figure 3

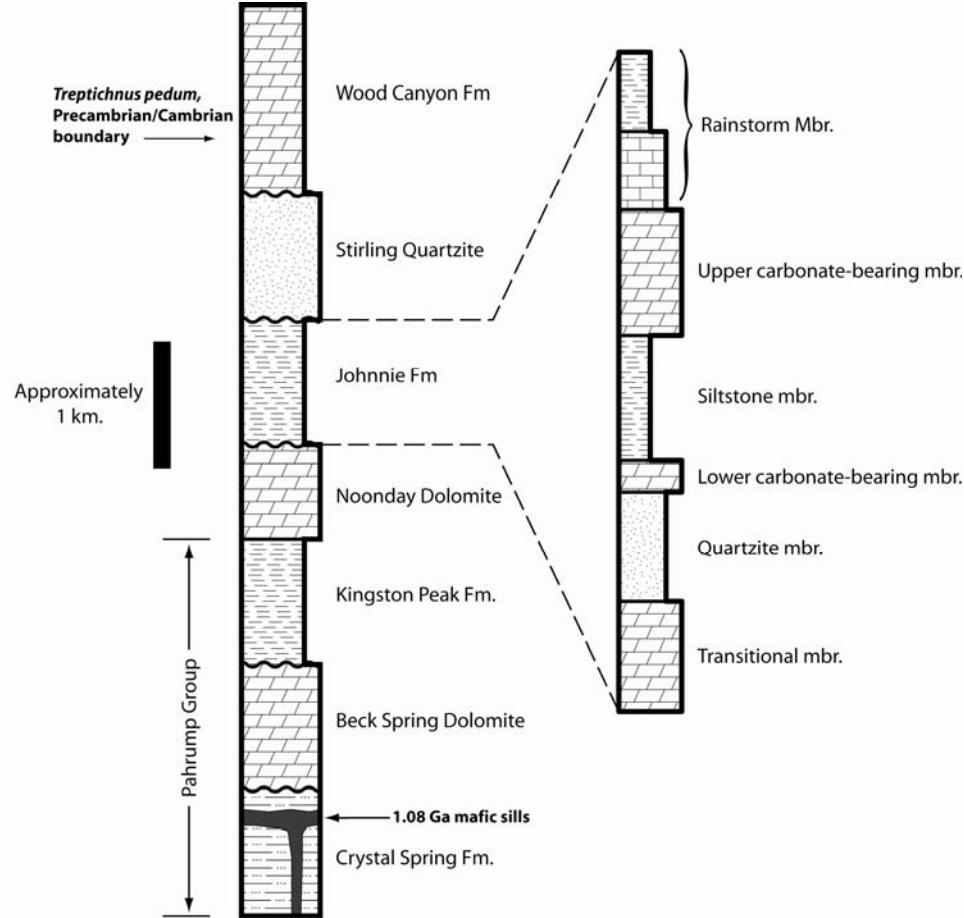


Figure 4

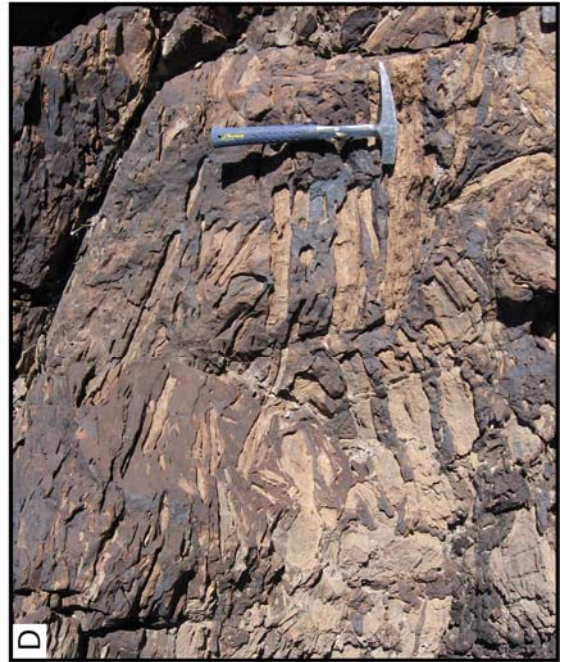
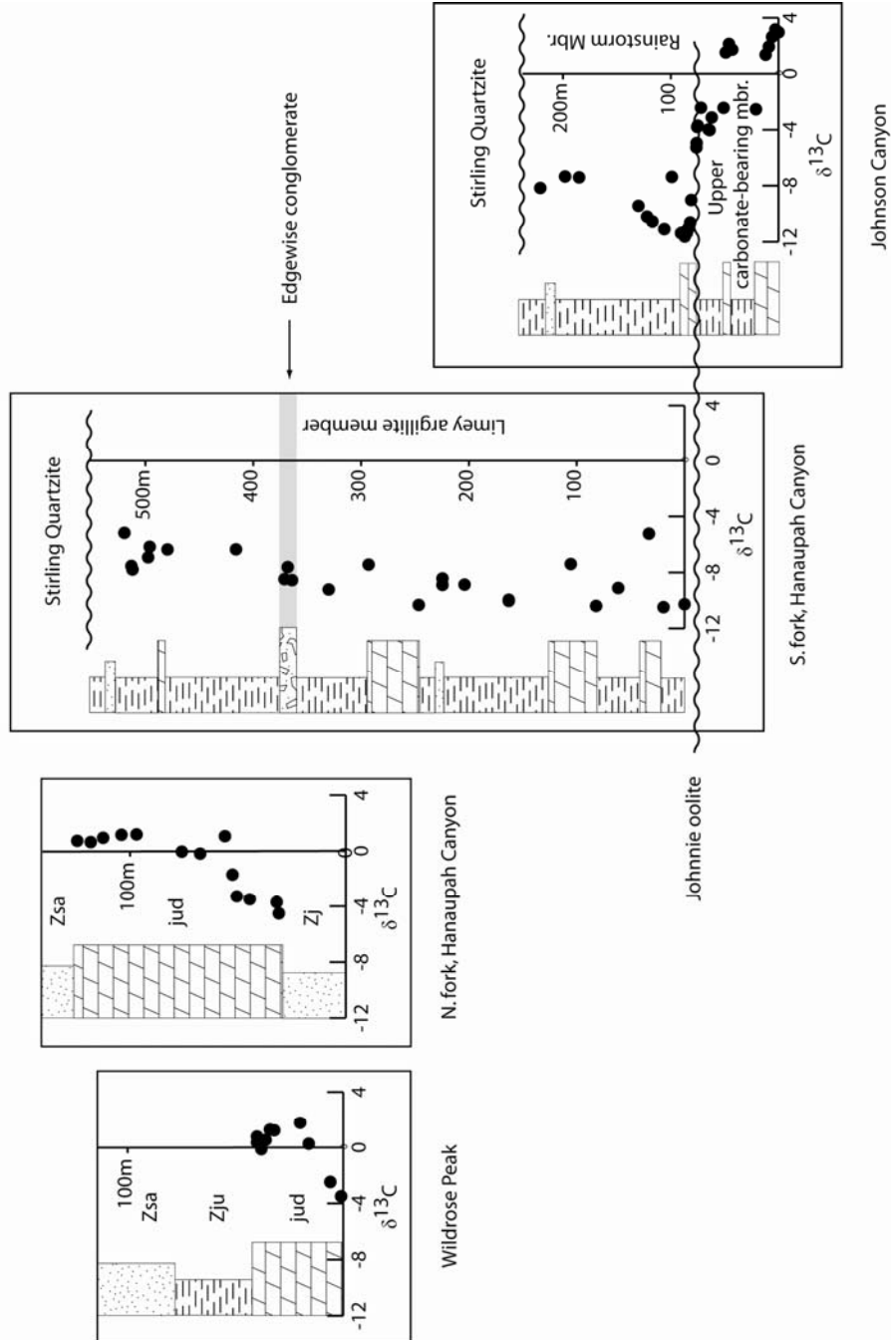


Figure 5



**Figure 6**

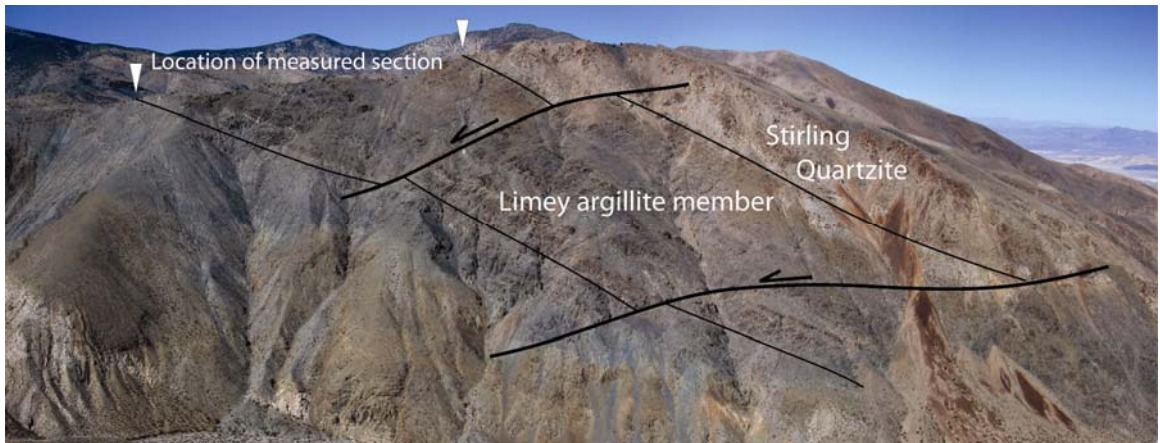


Figure 7

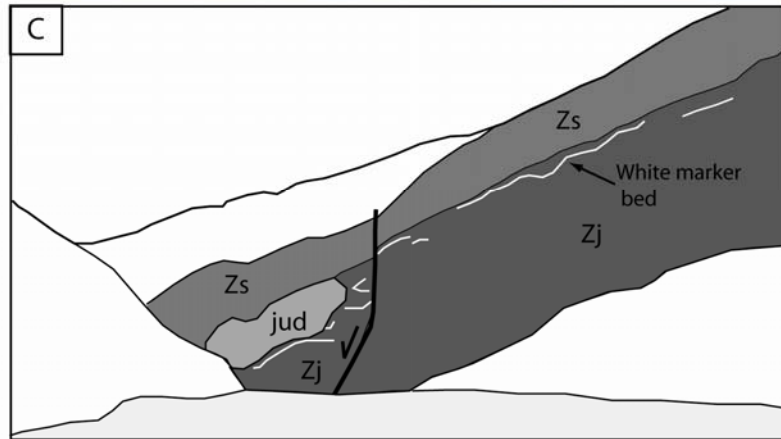
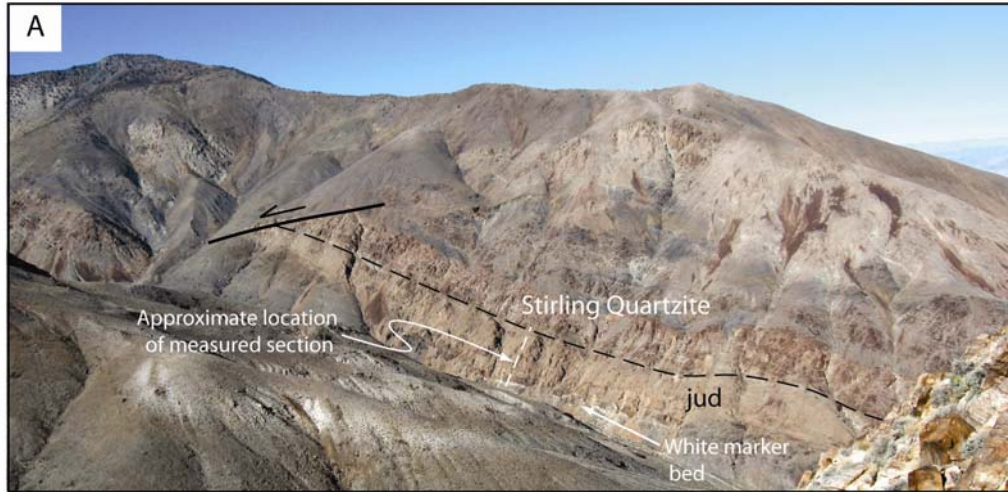


Figure 8

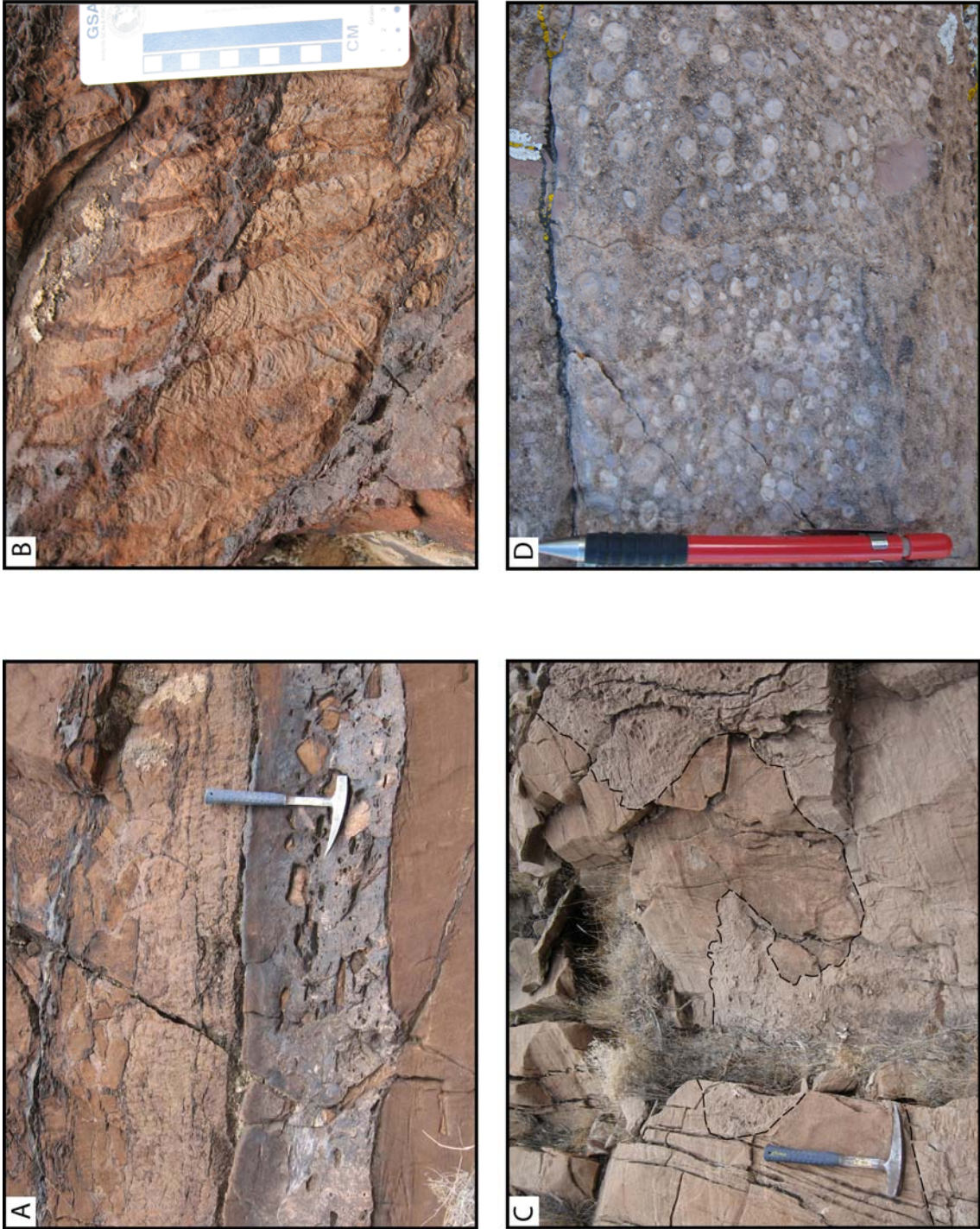


Figure 9

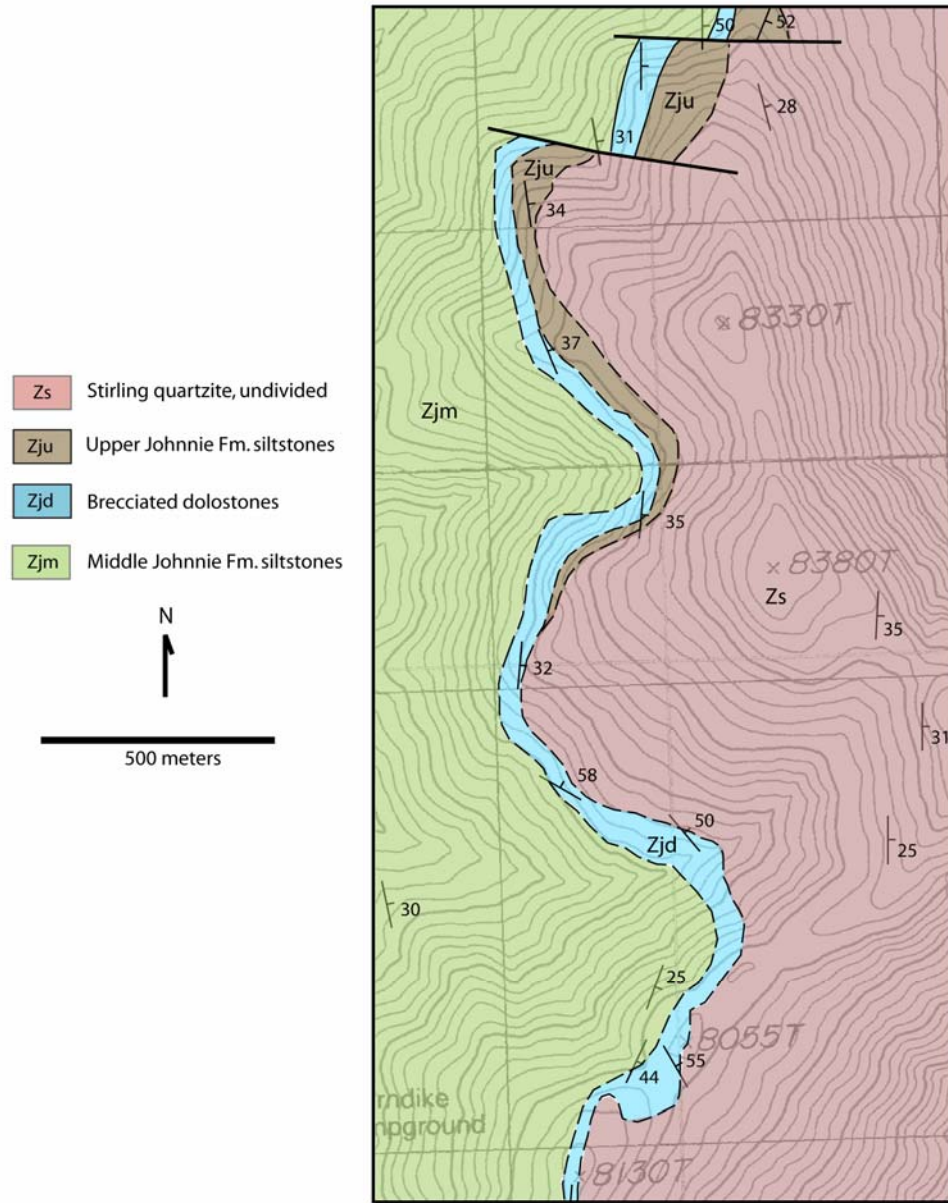


Figure 10

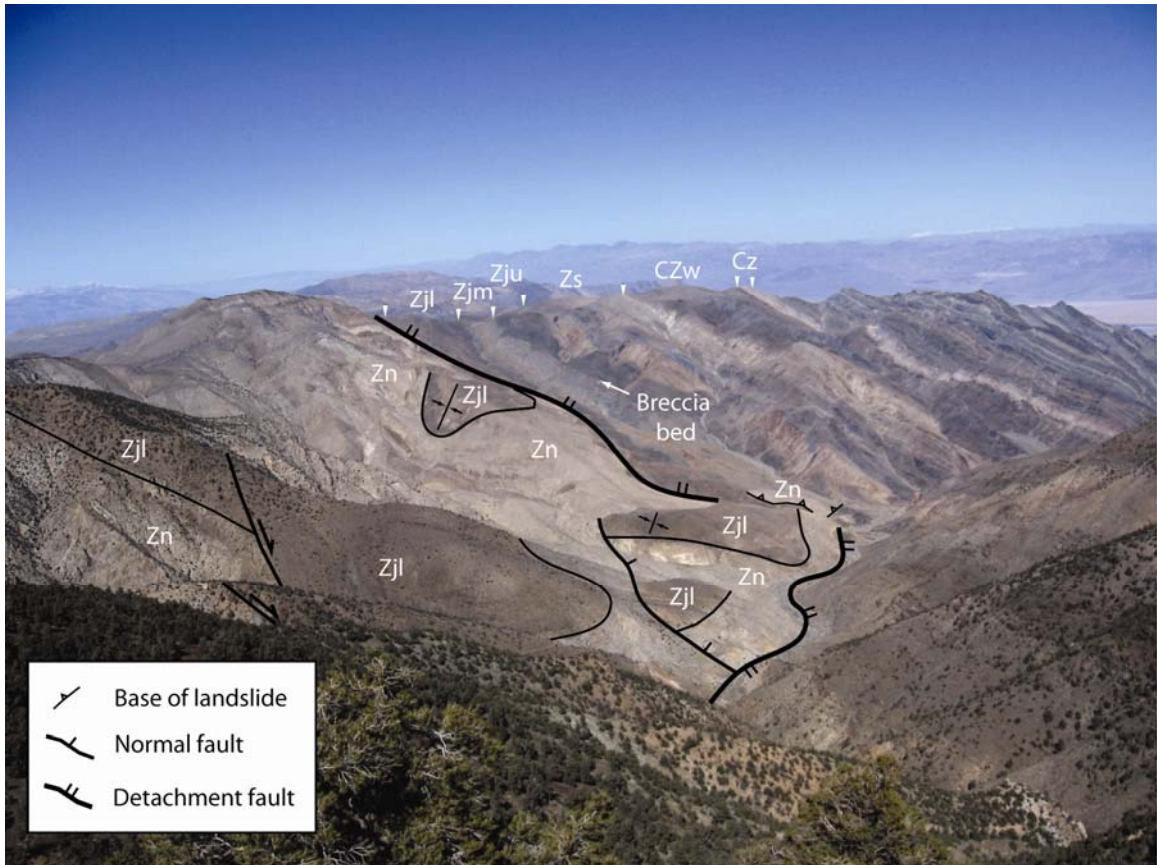


Figure 11

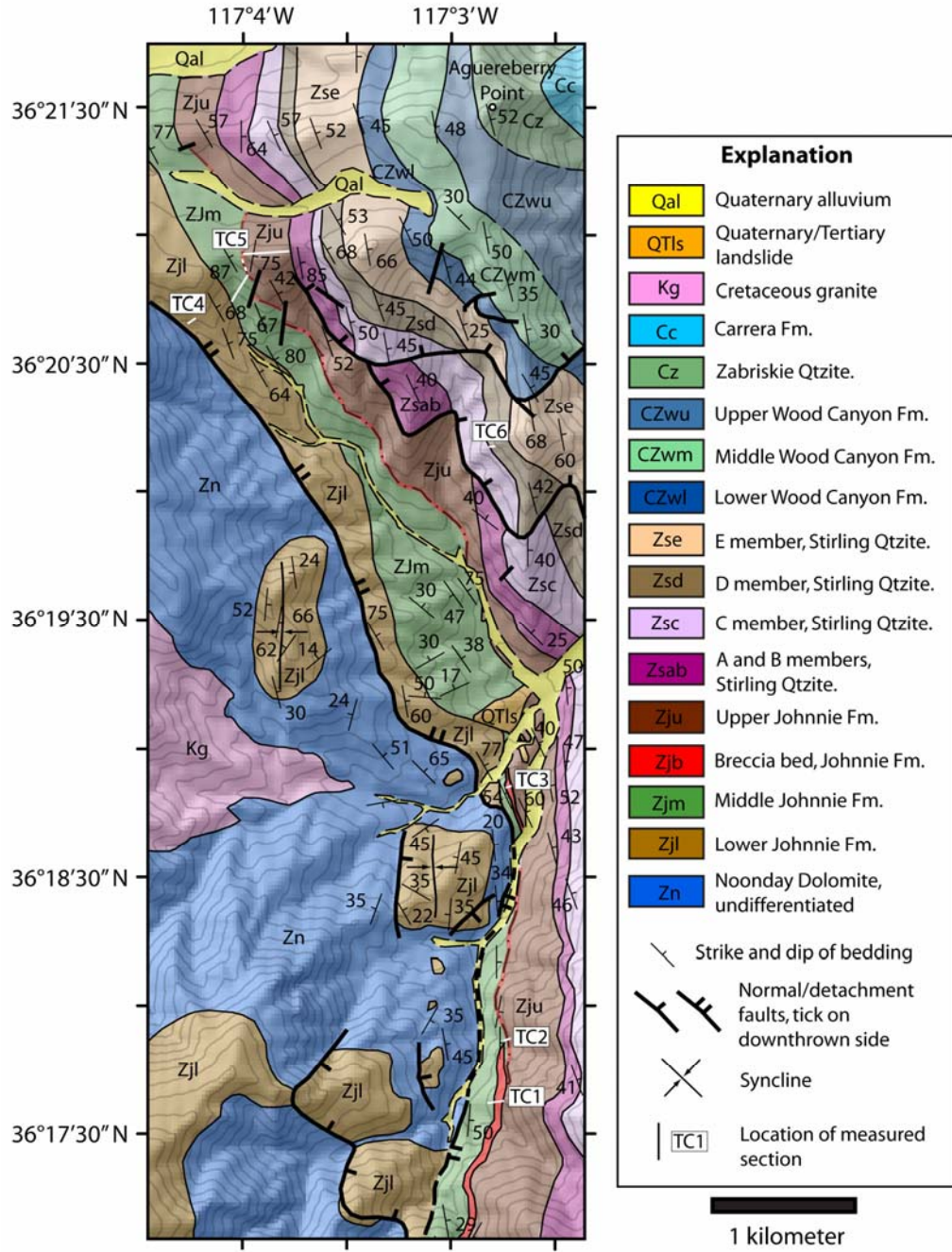


Figure 12



IV-58

**Figure 13**

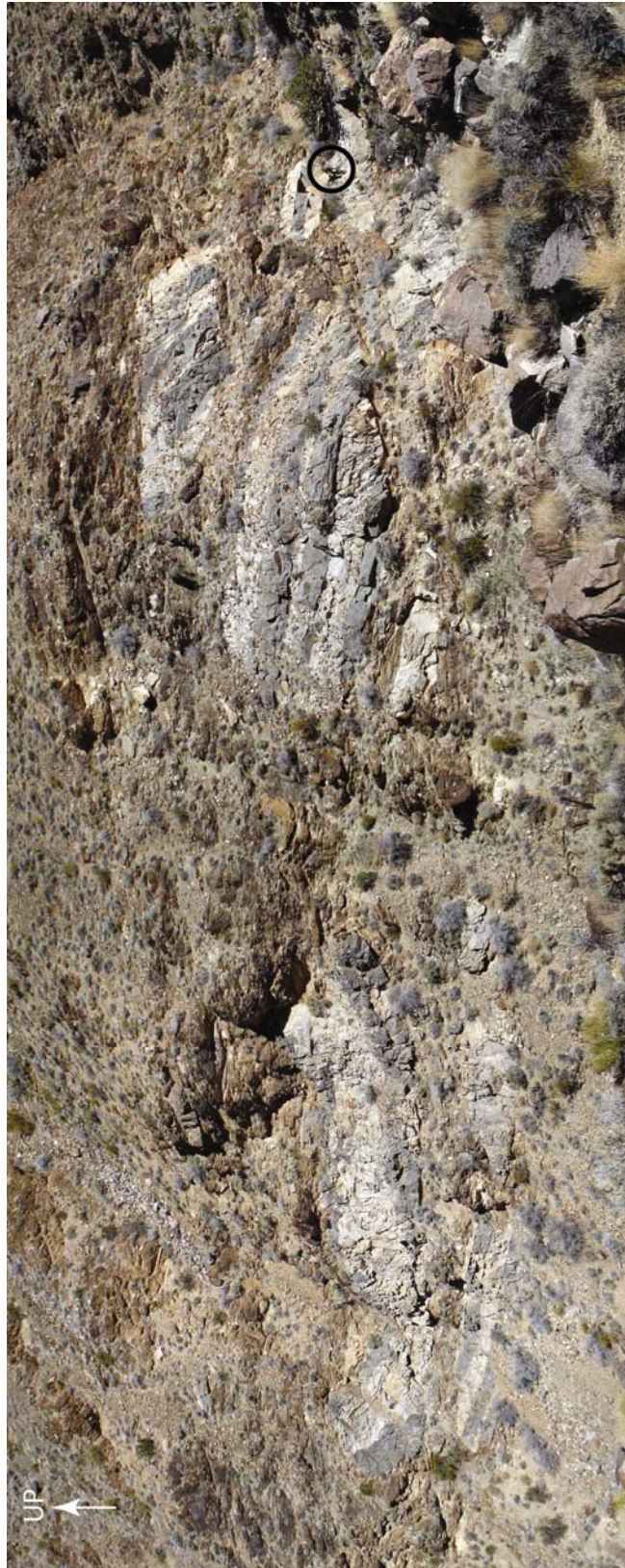


Figure 14

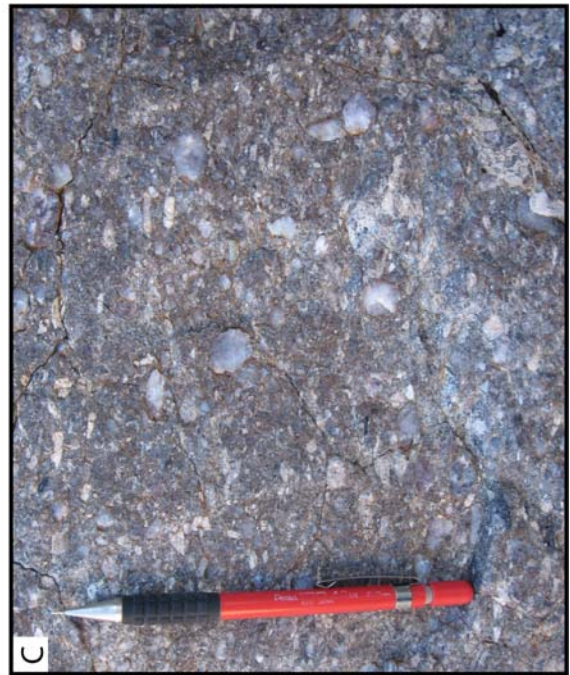
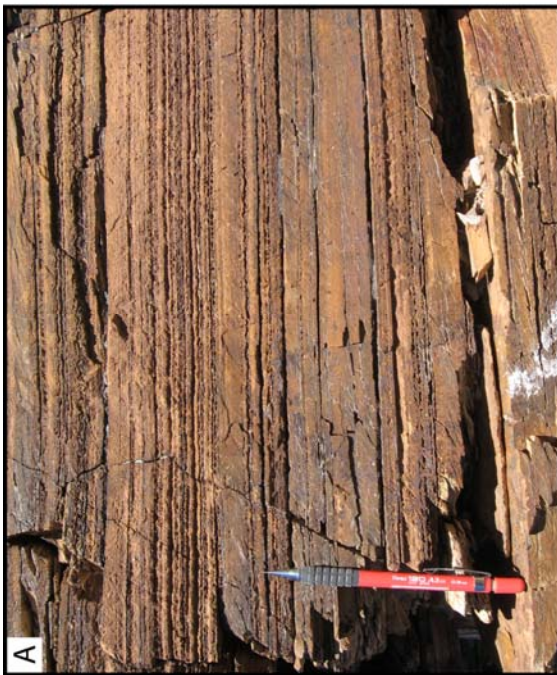


Figure 15

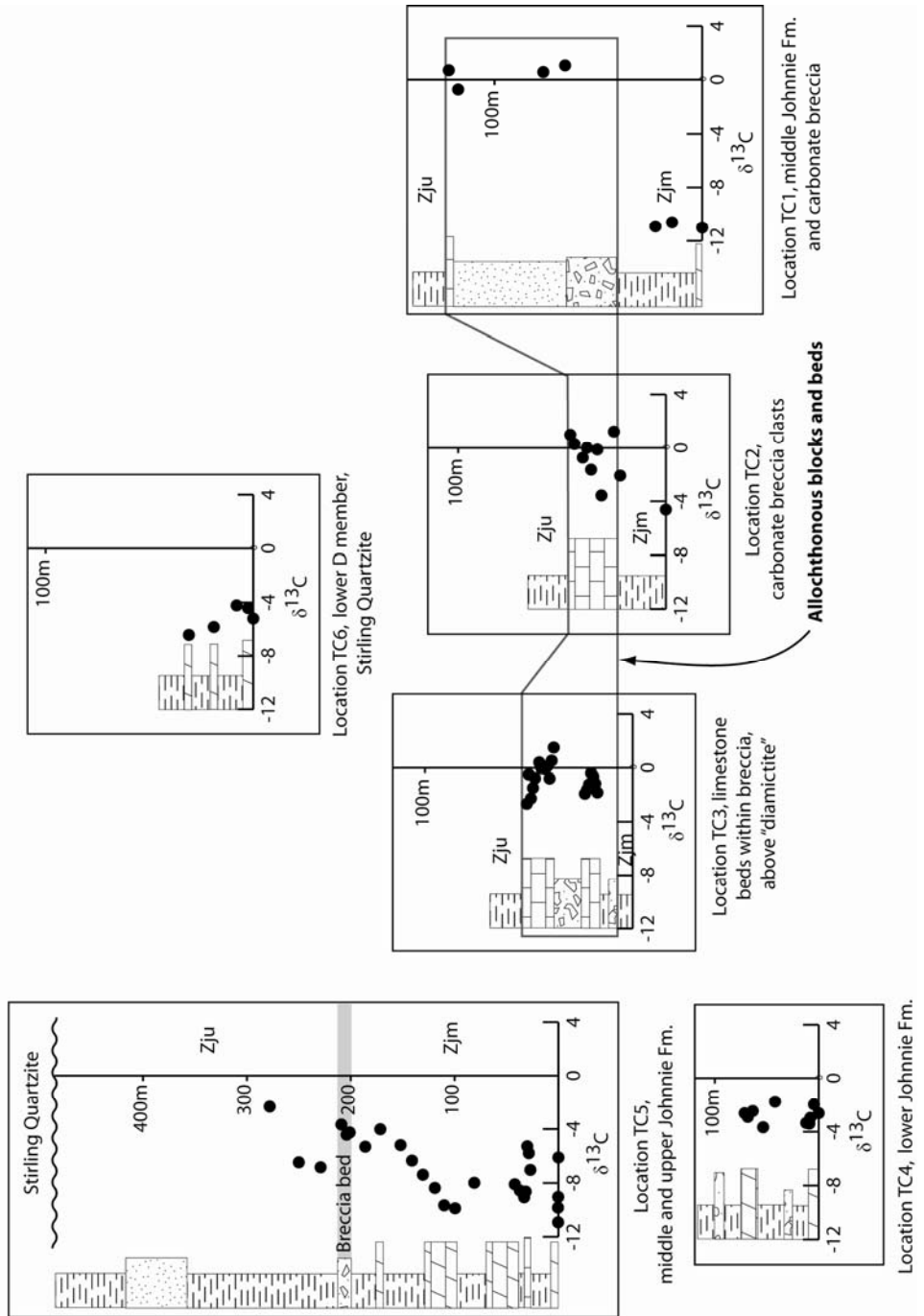


Figure 16

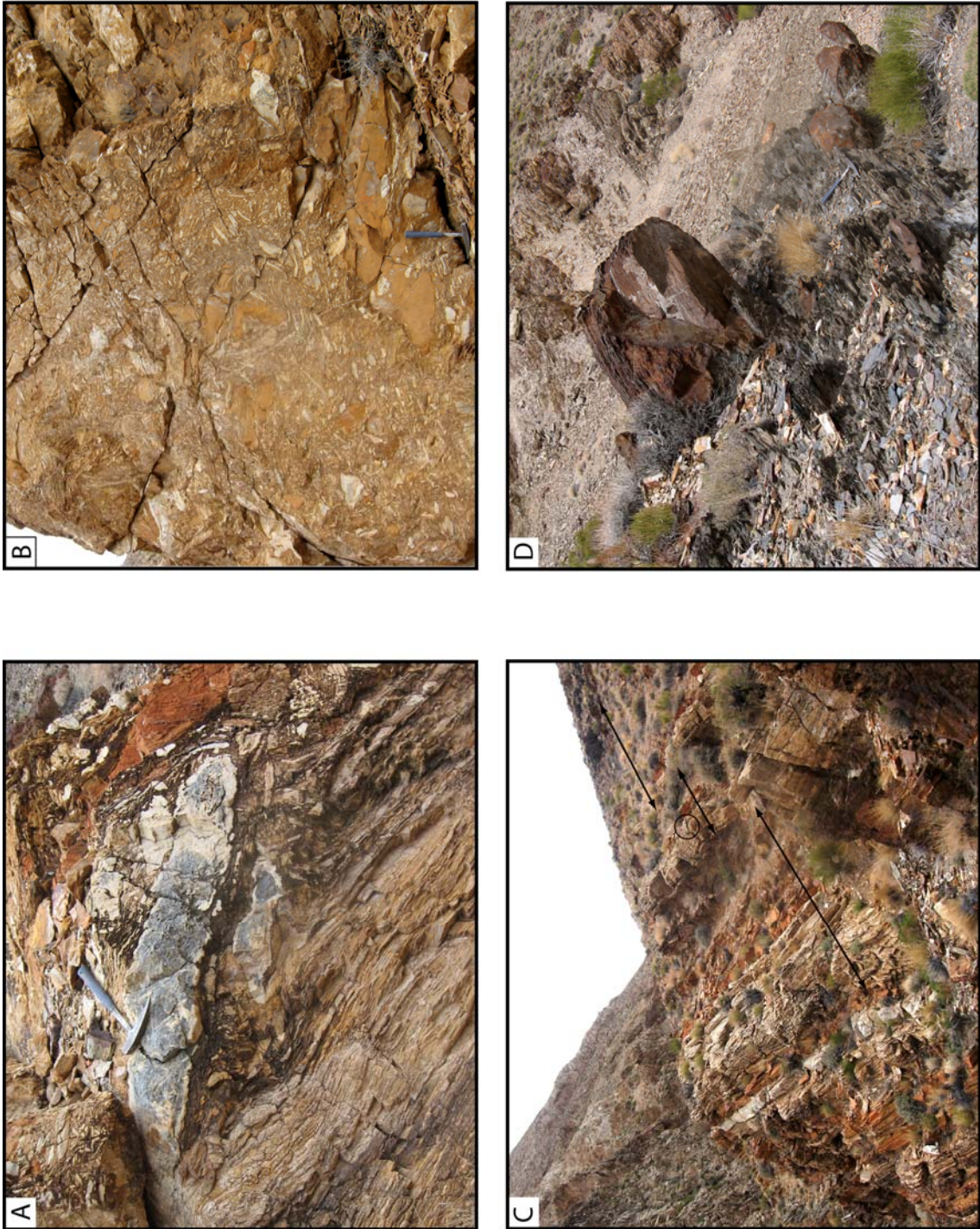


Figure 17

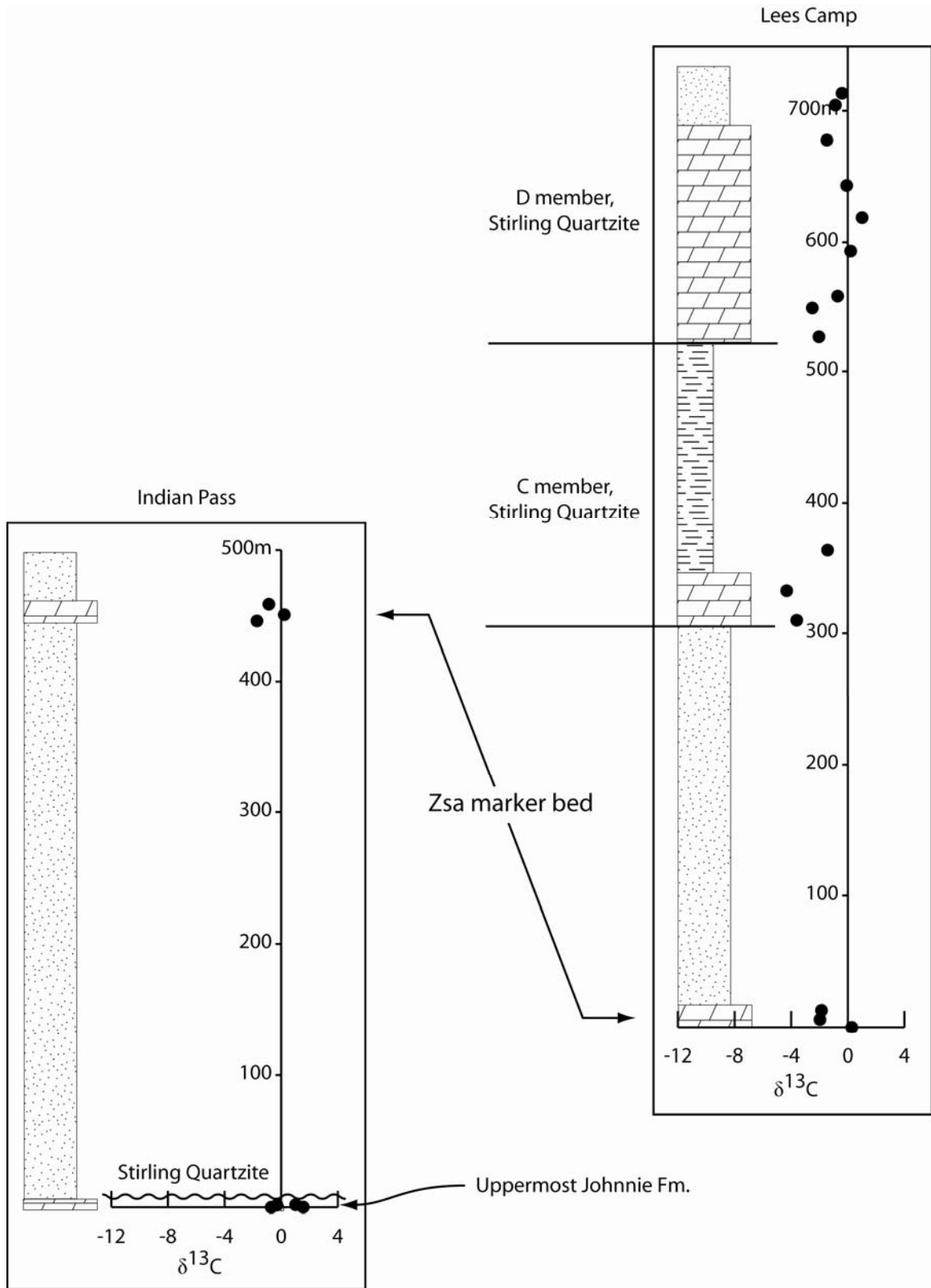


Figure 18

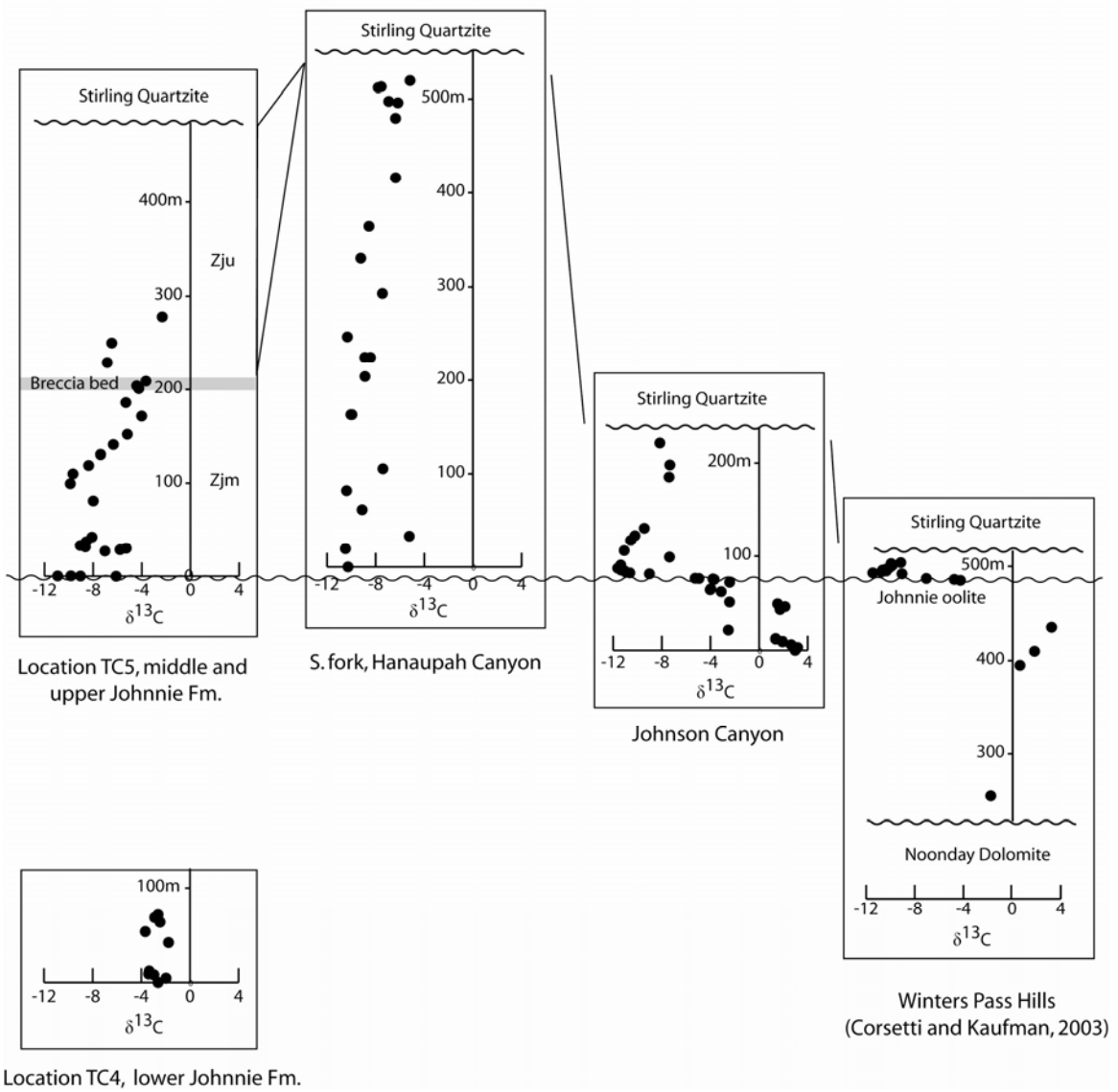


Figure 19

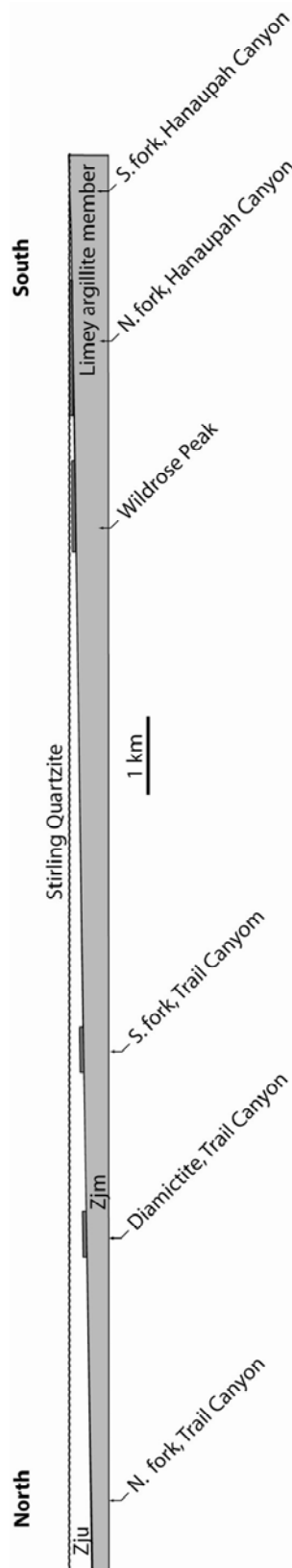
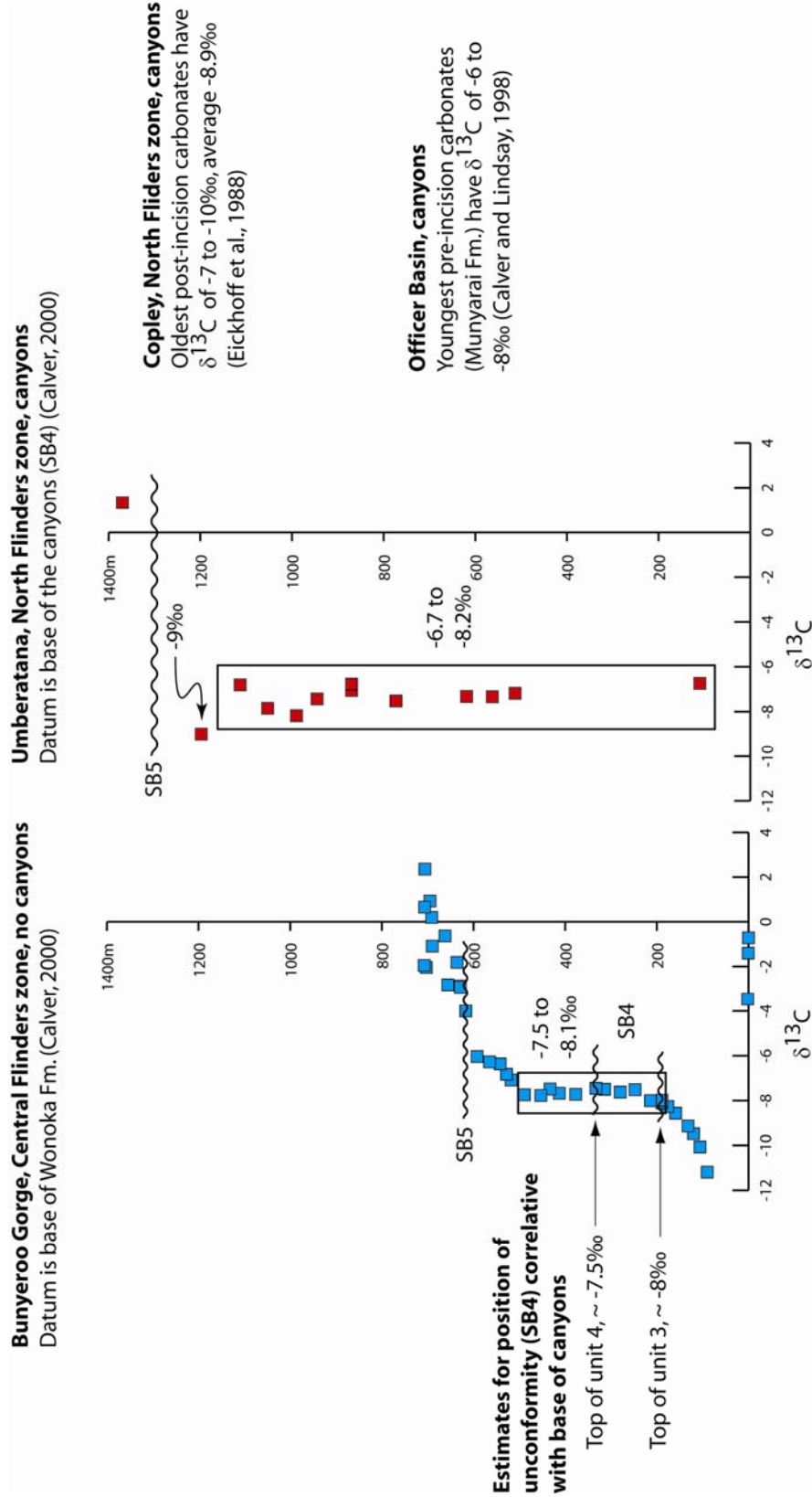


Figure 20



**Table 1: C and O isotope data tables**

<i>Johnson Canyon</i>				
<b>Sample</b>	<b>Stratigraphic position (m)</b>	<b>d<sup>13</sup>C<sub>PDB</sub></b>	<b>d<sup>18</sup>O<sub>PDB</sub></b>	<b>Notes</b>
JC1	0.0	2.96	-8.31	
JC2	3.0	3.16	-7.21	
JC3	6.0	2.63	-5.21	
JC4	9.0	1.93	-4.00	
JC5	12.0	1.36	-3.31	
JC6	21.0	-2.53	-7.12	
JC7	43.0	1.72	-8.97	
JC8	46.0	2.13	-6.14	
JC9	49.0	1.52	-5.26	
JC10	51.0	-2.43	-6.38	
JC11	62.0	-3.12	-9.58	
JC12	65.0	-3.97	-6.34	Break in section at prominent reddish brown dolostone below oolite
JC13	64.0	-4.02	-6.17	
JC14	72.0	-2.43	-10.47	
JC15	75.0	-3.70	-8.65	Base of Johnnie oolite
JC16	75.5	-3.80	-8.57	
JC17	76.0	-4.95	-8.55	
JC18	76.2	-5.26	-8.60	Top of Johnnie oolite
JC19	81.0	-9.02	-13.97	Base of pink limestones
JC20	82.0	-10.63	-15.87	
JC21	83.0	-10.99	-15.59	
JC22	84.0	-11.06	-14.73	
JC23	85.0	-11.35	-16.02	
JC24	87.0	-11.63	-16.04	
JC25	87.5	-11.47	-15.81	Top of pink limestones
JC26	90.5	-11.38	-15.45	
JC27	99.0	-7.37	-11.52	
JC28	106.0	-11.09	-16.26	
JC29	117.0	-10.56	-15.93	
JC30	122.0	-10.21	-15.54	
JC31	130.0	-9.44	-16.20	
JC32	185.0	-7.41	-12.35	
JC33	198.0	-7.34	-9.14	
JC34	221.0	-8.16	-9.60	Stirling contact at 235m

<i>South fork, Hanaupah Canyon</i>				
<b>Sample</b>	<b>Stratigraphic position (m)</b>	<b>d<sup>13</sup>C<sub>PDB</sub></b>	<b>d<sup>18</sup>O<sub>PDB</sub></b>	<b>Notes</b>
LA1	0.0	-10.27	-24.65	
LA2	19.5	-10.48	-19.91	
LA3	33.0	-5.23	-12.82	
LA4	61.5	-9.11	-22.50	
LA5	82.0	-10.39	-27.45	
LA6	105.5	-7.40	-15.97	
LA7	163.0	-10.03	-19.85	
HC1	163.0	-9.95	-18.77	
HC3	204.0	-8.87	-19.68	
HC4	224.5	-8.89	-18.88	
LA8	224.5	-8.43	-16.73	
HC5	246.5	-10.32	-17.50	
HC7	293.0	-7.44	-20.56	
LA9	330.0	-9.22	-21.49	
HC14	364.0	-8.55	-24.67	Base of edgewise conglomerate
HC13	368.0	-7.62	-20.67	Top of edgewise conglomerate
HC12	371.0	-8.48	-18.99	
HC8	416.0	-6.35	-29.49	
LA10	479.5	-6.36	-10.85	
LA11	497.5	-6.92	-12.02	
LA12	496.0	-6.17	-10.06	
LA13	512.0	-7.79	-12.05	
LA14	513.0	-7.54	-12.90	
LA15	519.5	-5.17	-9.04	Stirling contact at ~563m
<i>North fork, Hanaupah Canyon</i>				
<b>Sample</b>	<b>Stratigraphic position (m)</b>	<b>d<sup>13</sup>C<sub>PDB</sub></b>	<b>d<sup>18</sup>O<sub>PDB</sub></b>	<b>Notes</b>
CVNHC1	31.0	-4.51	-11.05	White marker bed at 22 to 27.5m
CVNHC5	32.0	-3.70	-8.46	
CVNHC2	44.5	-3.49	-7.52	
CVNHC3	50.5	-3.27	-8.87	
CVNHC4	52.5	-1.70	-6.36	
CVNHC6	56.0	1.06	-8.58	
CVNHC7	67.5	-0.19	-4.57	
CVNHC8	76.0	-0.05	-4.96	
CVNHC10	97.0	1.19	-4.00	
CVNHC11	104.0	1.16	-5.28	
CVNHC12	112.5	0.94	-7.75	
CVNHC13	118.3	0.63	-5.60	
CVNHC14	124.5	0.73	-4.35	Stirling contact at 126m

*Johnnie upper dolostone, near Wildrose Peak*

<b>Sample</b>	<b>Stratigraphic position (m)</b>	<b>d<sup>13</sup>C<sub>PDB</sub></b>	<b>d<sup>18</sup>O<sub>PDB</sub></b>	<b>Notes</b>
PM23	1.0	-3.49	-7.44	
PM32	6.0	-2.47	-6.81	
PM33	16.0	0.27	-5.52	
PM34	20.0	1.78	-3.19	
PM28	32.0	1.23	-5.46	
PM29	34.0	1.28	-5.02	
PM30	36.0	0.54	-7.37	
PM31	38.0	-0.12	-7.34	
PM27	40.0	0.36	-6.71	
PM35	40.0	0.78	-3.93	

*TC1*

<b>Sample</b>	<b>Stratigraphic position (m)</b>	<b>d<sup>13</sup>C<sub>PDB</sub></b>	<b>d<sup>18</sup>O<sub>PDB</sub></b>	<b>Notes</b>
PM73	0.0	-11.01	-17.07	
PM74	14.5	-10.62	-16.37	
PM75	22.5	-10.92	-16.28	
PM76	66.0	1.06	-11.56	Zjm/breccia contact at ~39m
PM77	76.5	0.57	-13.29	
PM78	117.5	-0.73	-12.34	
PM79	122.0	0.70	-9.05	Breccia/Zju contact at ~122.5m

*TC2*

<b>Sample</b>	<b>Stratigraphic position (m)</b>	<b>d<sup>13</sup>C<sub>PDB</sub></b>	<b>d<sup>18</sup>O<sub>PDB</sub></b>	<b>Notes</b>
PM37	0.0	-4.62	-15.63	Dolostone in Zjm
PM38	22.0	-2.08	-10.99	Dolostone in Zjm
PM39	25.0	1.22	-12.29	Lower block
PM40	31.0	-3.56	-14.20	Base of upper block
PM41	33.0	-0.12	-14.03	
PM42	36.0	-1.63	-14.15	
PM43	38.0	0.00	-11.32	
PM44	40.0	-0.73	-12.81	
PM45	44.0	0.29	-12.85	
PM46	46.0	0.98	-13.49	Top of upper block

<i>TC3</i>				
<b>Sample</b>	<b>Stratigraphic position (m)</b>	<b>d<sup>13</sup>C<sub>PDB</sub></b>	<b>d<sup>18</sup>O<sub>PDB</sub></b>	<b>Notes</b>
TC2	17.0	-1.82	-13.88	Base of blue-grey limestone
TC3	18.0	-1.17	-14.34	
TC4	19.0	-0.65	-14.81	
TC5	20.0	-0.38	-13.37	
TC6	21.0	-1.22	-13.71	
TC7	22.0	-1.62	-14.61	
TC8	23.0	-1.92	-13.98	1m below top of blue-grey limestone
TC9	38.0	1.50	-14.12	Base of black limestone
TC10	39.0	0.53	-14.03	
TC11	40.0	-0.79	-11.50	
TC12	41.0	0.13	-13.20	
TC13	42.0	-0.08	-14.13	
TC14	43.0	0.03	-14.48	
TC15	44.0	-0.02	-14.19	
TC16	45.0	0.40	-14.60	
TC17	47.0	-0.77	-13.67	
TC18	48.0	-1.48	-13.58	
TC19	49.0	-2.26	-13.18	
TC20	50.0	-0.49	-15.31	
TC21	51.0	-2.66	-13.58	Top of black limestone
<i>TC4</i>				
<b>Sample</b>	<b>Stratigraphic position (m)</b>	<b>d<sup>13</sup>C<sub>PDB</sub></b>	<b>d<sup>18</sup>O<sub>PDB</sub></b>	<b>Notes</b>
JL1	0.0	-2.62	-12.70	
JL2	4.5	-1.97	-11.87	
JL3	8.0	-2.96	-14.64	
JL4	9.0	-3.40	-13.46	
JL5	12.0	-3.35	-13.31	
JL6	42.0	-1.76	-16.72	
JL7	53.5	-3.67	-14.81	
JL8	63.5	-2.46	-13.53	Near base of deepening-upward cycles
JL9	68.3	-2.90	-13.23	
JL10	71.3	-2.62	-13.60	

<i>TC5</i>				
<b>Sample</b>	<b>Stratigraphic position (m)</b>	<b>d<sup>13</sup>C<sub>PDB</sub></b>	<b>d<sup>18</sup>O<sub>PDB</sub></b>	<b>Notes</b>
AP1	0.0	-6.11	-11.42	Base of Zjm
AP2	0.2	-9.04	-12.21	
AP3	0.3	-10.92	-12.79	Oolitic dolostone
AP4	0.4	-9.83	-12.36	Oolitic dolostone
AP5	27.0	-7.03	-11.61	
AP6	28.5	-5.79	-10.16	
AP7	30.0	-5.28	-10.78	
AP8	31.5	-8.64	-12.72	Pink, thin-bedded limestone
AP9	33.0	-9.06	-15.64	Pink, thin-bedded limestone
AP10	37.0	-8.57	-13.45	Pink, thin-bedded limestone
AP11	42.0	-8.10	-13.77	
AP12	81.0	-7.99	-13.07	
AP13	99.5	-9.88	-14.53	
AP14	110.0	-9.66	-15.47	
AP15	119.0	-8.37	-13.67	
AP16	130.5	-7.39	-13.15	
AP17	141.0	-6.34	-13.84	
AP18	152.0	-5.19	-11.72	
AP19	171.5	-4.01	-7.84	
AP20	186.0	-5.31	-11.35	
AP21	201.0	-4.25	-11.46	Pink thin-bedded dolostone at base of breccia interval
AP22	204.0	-4.42	-11.71	
AP23	209.0	-3.66	-9.16	Dolostone at top of breccia
AP24	229.0	-6.84	-11.39	
AP25	250.0	-6.47	-11.22	
AP26	278.0	-2.32	-3.42	Stirling contact at ~490m
<i>TC6</i>				
<b>Sample</b>	<b>Stratigraphic position (m)</b>	<b>d<sup>13</sup>C<sub>PDB</sub></b>	<b>d<sup>18</sup>O<sub>PDB</sub></b>	<b>Notes</b>
SD1	0.0	-5.20	-11.31	At base of Stirling D member
SD2	2.5	-4.42	-8.39	
SD3	8.0	-4.22	-11.30	
SD4	19.0	-5.83	-7.97	
SD5	31.0	-6.42	-12.31	
<i>Indian Pass</i>				
<b>Sample</b>	<b>Stratigraphic position (m)</b>	<b>δ<sup>13</sup>C<sub>PDB</sub></b>	<b>δ<sup>18</sup>O<sub>PDB</sub></b>	<b>Notes</b>
FM1	0.0	-0.70	-13.55	Upper Johnnie Fm.
FM2	0.2	1.56	-14.30	Upper Johnnie Fm.
FM3	1.7	-0.30	-14.20	Upper Johnnie Fm.
FM4	2.0	1.02	-10.24	Upper Johnnie Fm.
IP1	446.0	-1.71	-15.29	Stirling A member marker bed
IP2	450.8	0.22	-13.54	Stirling A member marker bed
IP3	458.8	-0.87	-7.07	Stirling A member marker bed

*Lees Camp*

<b>Sample</b>	<b>Stratigraphic position (m)</b>	$\delta^{13}\text{C}_{\text{PDB}}$	$\delta^{18}\text{O}_{\text{PDB}}$	<b>Notes</b>
LC1	0.0	0.28	-5.45	Stirling A member marker bed
LC2	6.0	-1.97	-5.71	Stirling A member marker bed
LC3	13.0	-1.86	-3.62	Stirling A member marker bed
LC4	310.0	-3.61	-2.54	Base of Stirling C member
LC5	332.5	-4.32	-5.41	
LC6	363.5	-1.43	-4.71	
LC7	526.5	-2.04	-7.14	Base of Stirling D member
LC8	548.5	-2.51	-10.29	
LC9	557.5	-0.72	-6.19	
LC10	592.5	0.20	-5.61	
LC11	618.0	1.01	-4.62	
LC12	642.5	-0.08	-7.99	
LC13	677.0	-1.48	-7.28	
LC14	703.5	-0.88	-7.70	
LC15	712.5	-0.41	-8.52	